

**Proteometabolomic characterization of apical bud maturation in *Pinus pinaster***

Journal:	<i>Tree Physiology</i>
Manuscript ID	TP-2020-237.R2
Manuscript Type:	Research Paper
Date Submitted by the Author:	n/a
Complete List of Authors:	Valledor, Luis; University of Oviedo, Organisms and Systems Biology Guerrero, Sara; University of Oviedo, Organisms and Systems Biology García-Campa, Lara; University of Oviedo, Organisms and Systems Biology Meijon, Monica; Universidad de Oviedo, Organisms and Systems Biology
Keywords:	Bud aging, Metabolomics, Proteomics, Integrative approach, Conifer

SCHOLARONE™  
 Manuscripts

1 **Title:** Proteometabolomic characterization of apical bud maturation in

2 *Pinus pinaster*

3  
4 **Running Title:** Proteometabolomic characterization of apical bud

5  
6  
7 Luis Valledor\*, Sara Guerrero, Lara García-Campa, Mónica Meijón\*

8  
9 Plant Physiology, Department of Organisms and Systems Biology, University of

10 Oviedo, Oviedo 33071, Asturias, Spain

11 \*Corresponding authors: [valledorluis@uniovi.es](mailto:valledorluis@uniovi.es); [meijonmonica@uniovi.es](mailto:meijonmonica@uniovi.es)

12  
13  
14  
15 **KEYWORDS:** Conifer, Bud aging, Metabolomics, Proteomics, Integrative approach

16  
17 **Number of words:** 10647

18 **Number of words:** 6555 (without References, Funding, Acknowledgments)

19 **Number of figures included in manuscript:** 5

20 **Number of Supplementary figures:** 1 (S1)

21 **Number of Supplementary tables:** 5 (S1 to S5)

22

1  
2  
3 23 **ABSTRACT (300 words)**  
4

5 24 Bud maturation is a physiological process which implies a set of morphophysiological changes  
6 25 which lead to the transition of growth patterns from young to mature. This transition defines tree  
7 26 growth and architecture, and in consequence traits such as biomass production and wood quality.  
8 27 In *Pinus pinaster*, a conifer of great timber value, bud maturation is closely related to polycyclism  
9 28 (multiple growth periods per year). This process causes a lack of apical dominance, and  
10 29 consequently increased branching that reduces its timber quality and value. However, despite its  
11 30 importance, little is known about bud maturation. In this work, proteomics and metabolomics were  
12 31 employed to study apical and basal sections of young and mature buds in *P. pinaster*. Proteins  
13 32 and metabolites in samples were described and quantified using (n)UPLC-LTQ-Orbitrap. The  
14 33 datasets were analyzed employing an integrative statistical approach, which allowed the  
15 34 determination of the interactions between proteins and metabolites and the different bud sections  
16 35 and ages. Specific dynamics of proteins and metabolites such as HISTONE H3 and H4,  
17 36 RIBOSOMAL PROTEINS L15 and L12, CHAPERONIN TCP1, 14-3-3 protein gamma,  
18 37 gibberellins A1, A3, A8, strigolactones and ABA, involved in epigenetic regulation, proteome  
19 38 remodeling, hormonal signaling and abiotic stress pathways showed their potential role during  
20 39 bud maturation. Candidates and pathways were validated employing interaction databases and  
21 40 targeted transcriptomics. These results increase our understanding of the molecular processes  
22 41 behind bud maturation a key step towards improving timber production and natural pine forests  
23 42 management in a future scenario of climate change. However, further studies are necessary by  
24 43 using different *P. pinaster* populations that show contrasting wood quality and stress tolerance in  
25 44 order to generalize the results.  
26 45

## 46 INTRODUCTION

47 Pines are key players of forest ecosystems since most species have the ability to colonize a great  
48 variety of niches, act as good CO<sub>2</sub> sinks due to its fast growth (Allona et al., 1998), and are  
49 demanded by forest industry due to their quality timber, paper pulp and resins (Canales et al.,  
50 2014). Current production is not enough to cover current and predicted timber demand (FAO,  
51 2009) and new strategies should be designed for implementing a more sustainable forest  
52 management also considering the climate change scenario (FAO, 2015). The use of fast-growth  
53 species such as *Pinus pinaster* Aiton, commonly known as maritime pine, may have an important  
54 role to this aim. This species has a major ecological and industrial role in southern Europe both  
55 at Mediterranean and Atlantic basins (González et al., 2016; Meijón et al., 2016; Cano et al.,  
56 2018). Its provenances adapted to different geoclimatic conditions across its distribution exhibit  
57 specific adaptations, allowing its optimal growth under a wide range of environments, from mild  
58 humid Atlantic regions to warm dry Mediterranean. These adaptations are genetically encoded,  
59 having this species a great genetic variability (Meijón et al., 2016; Vizcaíno-Palomar et al., 2016;  
60 Vázquez-González et al., 2019).

61 However, the architecture of this species can be greatly affected by harsh environmental  
62 conditions like drought periods, which can ultimately affect tree productivity. *Pinus pinaster* is a  
63 species with a characteristic polycyclic growth (multiple shoot flushes in a single season) (Zas et  
64 al., 2004). This growth pattern, which reduces tree value due to a loss of apical dominance and  
65 increased branching, is inheritable and genetically conditioned, with provenances more polycyclic  
66 than others (Sabatier et al., 2003; Zas et al., 2004; Meijón et al., 2016). Polycyclism also presents  
67 an important environmental component, being conditioned by water availability, soil composition  
68 or radiation (Sabatier et al., 2003; Girard et al., 2011). It has been shown that periods of drought  
69 reduce its appearance and also tree growth, and that fertile soils and good irradiation lead to  
70 increase growth cycles and branching (Sabatier et al., 2003; Verdú and Climent, 2007).  
71 Polycyclism is also conditioned by the maturation state of the apical bud (Sabatier et al., 2003;  
72 Girard et al., 2011), being buds with young phenology more polycyclic than mature, although the  
73 molecular mechanisms that explain these differences have not yet been described.

74 Bud maturation implies a number of phenological changes, altering growth pattern,  
75 morphogenetic competence and increasing abiotic stress resistance (Jordy, 2004; Brunner et al.,  
76 2017). Maturation is regulated by internal and environmental factors. Among internal factors, plant  
77 hormones (Meijón et al., 2009) and epigenetic mechanisms regulating differential gene  
78 expression are required for bud maturation (Valledor et al., 2010b; Valledor et al., 2015; Conde  
79 et al., 2017). This differential gene expression should lead to changes in proteome and, in  
80 consequence, in metabolome, altogether resulting in the physiological and morphological  
81 characteristics of each ontogenetic age (Haffner et al., 1991; Meijón et al., 2016; Großkinsky et  
82 al., 2017). Surprisingly, and despite its importance for adaptive responses, tree growth or  
83 polycyclism, little is known about the molecular processes that are behind bud maturation process  
84 and different developmental stages and how they interact with environment. The great complexity

1  
2  
3 85 that these processes seem to have along with the large number of variables potentially involved  
4 86 and not previously described suggest an unmanaged and massive strategy as the most  
5  
6 87 appropriate to address this problem.  
7

8 88 The availability of high throughput alternatives for molecular phenotyping such as gel-free  
9 89 proteomics and metabolomics give us an unprecedented capability to address this gap (Valledor  
10 90 et al., 2018). These techniques usually associated to model species can currently be applied with  
11 91 high confidence in almost any organism, since they do not require extended genome information.  
12 92 Despite unsequenced, *Pinus pinaster* has extensive transcriptomic data available that ease  
13 93 protein identification (Romero-Rodríguez et al., 2014). In this species, there are several  
14 94 contributions in the proteomics field but focused on the study of wood forming tissues (Paiva et  
15 95 al., 2008; Garcés et al., 2014) and somatic embryogenesis (Morel et al., 2014; Trontin et al.,  
16 96 2016). As the final reflection of genomes and its variation, metabolome analyses allowed to define  
17 97 population structures and evolution in this species (Meijón et al., 2016; López-Goldar et al., 2019),  
18 98 and also adaptive responses to abiotic/biotic stress (Cañas et al., 2015; de Simón et al., 2017;  
19 99 López-Goldar et al., 2020). The combination of different omics greatly increases the power of  
20 100 analysis since the datasets of the different levels complement each other in a synergistic way  
21 101 (Mochida and Shinozaki, 2011; Kim et al., 2012). This type of integrative studies has already been  
22 102 carried out successfully in conifers to study needle development combining proteomics and  
23 103 transcriptomics (Valledor et al., 2010a) or to comprehensively analyze response to heat  
24 104 (Escandón et al., 2017) or ultraviolet stress comparing proteomics and metabolomics (Pascual et  
25 105 al., 2017). However, there is no information related to bud maturation in pines.

26  
27 106 Therefore, the main aim of this work was to study the bud maturation process in *Pinus pinaster*  
28 107 using integrative omics approach combining proteomics and metabolomics. The integration of  
29 108 both levels allowed the extensive characterization of bud maturation processes. Specific  
30 109 dynamics of proteins and metabolites related to epigenetic regulation, proteome remodeling,  
31 110 hormonal signaling, and abiotic stress response (such as histones, ribosomal proteins,  
32 111 strigolactones, gibberellins, ABA, and chaperones) showed an essential role during bud  
33 112 maturation. In addition, the interconnection of these elements and its relation to different polycyclic  
34 113 capacity and stress tolerance of each maturation state of the bud was revealed through an  
35 114 integrative approach.

## 36 115 **MATERIAL AND METHODS**

### 37 116 **Plant material and growth conditions**

38 117 Apical buds in young and mature stages were sampled from two-years-old *Pinus pinaster*  
39 118 seedlings (plant size around  $20 \pm 3$  cm) just after they exhibited young/mature apical phase  
40 119 change. These plants were grown in a greenhouse with seasonal fertirrigation.

41 120 Buds in the young stage show leaf primordia differentiate into photosynthetically active primary  
42 121 needles around of the shoot apical meristem (SAM). However, when the mature stage is reached,

1  
2  
3 122 leaf primordia differentiate into scale leaves, and photosynthetic activity is shifted to long needles  
4 123 differentiated on brachyblasts in more distal positions on the stem (Jordy, 2004). Apical buds of  
5 124 18 seedlings of the same age, half of them having mature morphology and half of them young,  
6 125 were sampled and dissected into their apical and basal sections, corresponding to apical and  
7 126 axillary/foiar meristems, respectively (Figure 1). Three biological replicates for each treatment  
8 127 (apical and basal parts of the bud, young and mature buds) were constituted pooling basal or  
9 128 apical parts of the buds of three different seedlings with the same bud developmental stage.  
10 129 Samples were immediately frozen in liquid nitrogen and kept at -80 ° C until biomolecule  
11 130 extraction. Metabolites, proteins, and RNA were isolated from the same sample following the  
12 131 protocol of Valledor et al. (2014a) using 75 mg of fresh weight per sample.

### 132 **Metabolome analysis**

133 High-performance liquid chromatography (Dionex Ultimate 3000, ThermoFisher Scientific, USA)  
134 was coupled to a LTQ-Orbitrap XL high resolution mass spectrometer equipped with a HESI II  
135 (heated electrospray ionization) source and controlled by Xcalibur version 2.2 (Thermo Fisher  
136 Corporation). Polar fraction of each sample was analyzed twice, first using the positive and then  
137 the negative ion modes. Samples were run according to the procedure described by Meijón et al.  
138 (2016). Instrument was operated in full-scan mode with a resolution of 60 000, and spectra were  
139 acquired in mass range  $m/z$  50–1000 in the positive mode, and 65–1000 in the negative mode.  
140 The resolution and sensitivity were controlled by the injection of a standard mix (caffeine, proline,  
141 and sucrose) after the analysis of each batch and resolution was also checked with the aid of lock  
142 masses (phthalates). Blanks were also analyzed during the sequence. With the aim of improving  
143 metabolite assignation, one sample of each treatment was additionally reanalyzed including an  
144 ion fragmentation step. Chromatographic and analytical conditions were the same, but top-three  
145 ions of each scan were fragmented (30 s dynamic exclusion window). Parent ions (minimum  
146 intensity of 500) were fragmented by CID (normalized collision energy of 35, activation Q 0.25,  
147 and activation time 90 ms). These spectra were employed for MS/MS metabolite identification as  
148 described below.

149 RAW files were directly processed employing MZMINE v2.14 (Pluskal et al., 2010). Spectra were  
150 filtered establishing noise threshold at  $2 \times 10^4$  and minimum peak height at  $2.5 \times 10^5$ . Peaks were  
151 smoothed and deconvoluted using a local minimum search algorithm (95 % chromatographic  
152 threshold, minimum retention range 0.2 min, minimum relative height of 5 %, and minimum ratio  
153 top/edge of 0.5). Chromatograms were aligned using the RANSAC algorithm with a tolerance of  
154 5 ppm of  $m/z$  and 0.2 min of retention time. Peak areas were used for quantification.

155 Peaks were identified following a sequential approach. The first stage was performed against our  
156 in-house library (>100 compounds) and manual annotation considering its  $m/z$  and retention  
157 times. In a second stage, MS/MS data was used for identification employing Compound  
158 Discoverer software (Thermo Scientific, USA) and custom scripts for comparing experimental  
159 data to MS/MS databases Metlin, HMDB and FooDB. A positive identification was defined when

1  
2  
3 160 parent mass was below 5-ppm threshold compared to analyte in DB and at least, two main ions  
4 161 of fragmentation spectra were identified. The last stage assigned potential identity to masses by  
5 162 direct comparison of ion masses using a 5-ppm threshold and KEGG, HMDB, FooDB, Plantcyc,  
6 163 and MassBank databases. Those metabolites that were defined after the comparison with our  
7 164 standard compound library or by a matching of MS/ MS were considered as unquestionably  
8 165 'identified', while were considered 'tentatively assigned' those molecular ions with exact masses  
9 166 corresponding to identified metabolites in databases. Metabolite identification against our library  
10 167 was confirmed by RT, mass, and isotopic patterns.

## 15 168 **Protein identification and quantitation using nLC-Orbitrap-MS analysis**

16 169 Sixty µg of total protein were cleaned, digested, and desalted following the protocol described by  
17 170 Valledor and Weckwerth (2014). Peptide chromatography and mass spectrometric analysis were  
18 171 performed according to Pascual et al. (2017) with only a slight modification in the effective  
19 172 gradient, which was set to 90 min from 5 % to 45 % acetonitrile/0.1 % formic acid (v:v) with a later  
20 173 column regeneration step of 27 min. The employed column was a Chromolith RP-18R 15 cm  
21 174 length 0.1 cm inner diameter (Merck, Germany).

22 175 Spectra were processed in Proteome Discoverer 2.0 (Thermo Scientific, USA). Protein  
23 176 identification threshold was established at 5% and 1% false discovery rates (FDR) at peptide and  
24 177 protein levels, respectively. Only proteins with at least two identified peptides and one of them  
25 178 unique were considered as identified. Four databases were used: *Pinus sylvestris* and *Pinus*  
26 179 *taeda* (34063 accessions) (Proost et al., 2014), and against in-house databases, *Pinus pinaster*  
27 180 (117080 accessions) and *Pinus radiata* (67647 accessions) that were built following the  
28 181 procedure described by Romero-Rodríguez et al. (2014). Proteins were also functionally  
29 182 classified according to Mapman (Thimm et al., 2004) functional bins. Identified proteins were  
30 183 quantified by a label-free approach based on the estimation of the areas of the three most  
31 184 abundant peaks assigned to each protein by Proteome Discoverer.

## 32 185 **Targeted transcriptomic analysis of candidate genes**

33 186 RNA abundance was determined in a microdrop spectrophotometer NB1 (Nabi, South Korea) and  
34 187 its integrity was checked by agarose gel electrophoresis. One µg of RNA was reversed  
35 188 transcribed using the RevertAid kit (Thermo Scientific, USA) and random hexamers as primers  
36 189 following the manufacturer's instructions. qPCR reactions were performed in a CFX96™ Real-  
37 190 Time System (Biorad, USA) with RealQ Plus Master Mix Green, no ROX (2X) (Ampliqon,  
38 191 Denmark); four biological and two analytical replicates per treatment were made for each gene.  
39 192 Expression levels of *GLYCERALDEHYDE 3-PHOSPHATE DEHYDROGENASE (GAPDH)* and  
40 193 *UBIQUITINE (UBI)* were used as endogenous control and the results were analyzed by Bio-Rad  
41 194 CFX Manager 3.1 (Biorad, USA) software using the cycle threshold comparative method ( $\Delta C_T$ ).  
42 195 Detailed information about the primers used for qPCR experiments is available in Supplementary  
43 196 Table S1.

## 197 **Statistical and bioinformatics analysis**

198 All statistical procedures were conducted with the R programming language running under the  
199 open source computer software R v3.5.0 (R Development Core Team, 2015) and RStudio  
200 v1.1.423 (RStudio Team, 2016) using the packages pRocesomics<sup>1</sup> and mixOmics (Rohart et al.,  
201 2017).

202 Three biological replicates per treatment were used for metabolome and proteome analysis.  
203 Proteome and metabolome datasets were pre-processed following the recommendations of  
204 Valledor and Jorrín (2011) and Valledor et al. (2014b). In brief, missing values were imputed using  
205 a Random Forest approach, and variables were filtered out if they were not present in at least all  
206 of replicates corresponding to one treatment or in at least 45% of the analyzed samples. Data  
207 were normalized and transformed following a samplecentric approach followed by log  
208 transformation. Centered and scaled values (z-scores) were subjected to univariate (one-way  
209 ANOVA followed by a Tukey HSD post-hoc test, P<0.05.) and Venn diagrams, and heat map  
210 clustering. To avoid variable noise only those variables with interquartile range 50% greater than  
211 average were selected for multivariate analyses. Integrative analysis was based on the use of  
212 DIABLO algorithm and network representation. Cytoscape v. 3.7 (Shannon et al., 2003) was  
213 employed in network representation and analysis. Proteins were annotated according to Mapman  
214 classification employing protein sequences and Mercator online tool v3.6 (Lohse et al., 2014)  
215 while metabolites were manually classified according to this classification.

## 216 **RESULTS**

### 217 **Proteomic and metabolomic characterization of buds in *Pinus pinaster***

218 Proteomic analyses of young and mature buds and their sections allowed the identification of  
219 1609 proteins. Proteins were annotated according to Mapman, classifying 1540 proteins in 34  
220 functional bins. 951 proteins showed abundances and consistencies above threshold for their use  
221 in quantitative analyses. Out of these, 142 were differentially accumulated between treatments  
222 (ANOVA p-value <0.05; Supplementary Table S2). At metabolome level, 3670 peaks were  
223 detected, being 2267 suitable for quantification (Supplementary Table S3). From these, 133  
224 peaks were unequivocally identified using the in-house database or MS/MS spectra,  
225 corresponding to 105 unique compounds, and 974 were tentatively assigned by comparing their  
226 very accurate masses to those available in public databases (Supplementary Table S4). 75  
227 metabolites were classified according to Mapman. Despite the high number of identified/assigned  
228 metabolites, their complete classification according to Mapman was not possible, mainly due to  
229 the difficulty of classifying secondary metabolites. However, this potential bias does not affect the  
230 most studied and preserved functional groups such as those related to primary metabolism. From  
231 all detected compounds, 914 were differentially expressed between analyzed samples (ANOVA  
232 5% FDR; Supplementary Table S3).

---

<sup>1</sup> <https://github.com/Valledor/pRocesomics>



233 Venn analyses revealed qualitative differences between ontogenic stages and bud sections. At  
234 protein level (Figure 2A), young buds (apical and basal sections) showed the highest number of  
235 characteristic proteins (126) but, interestingly, the apical section of the mature bud was the most  
236 differentiated organ with 59 characteristic proteins. At metabolome level (Figure 2B), mature  
237 tissues showed the highest rate of unique compounds (569), while the apical section of the young  
238 bud exhibited the highest number of characteristic metabolites (194).

239 Quantitative analyses of Mapman classified proteins (Figure 2C) and metabolites (Figure 2D)  
240 pointed the differential pathways among bud sections and developmental stages. At proteome  
241 level, increased pathway clusters related to stress, hormone, lipidic, energetic, and major  
242 carbohydrate metabolism pathways can be correlated to the different tissues that were analyzed.  
243 Heatmap classified samples according to bud section, which may be suggesting a greater  
244 variation between apical and basal meristem proteomes than between mature and young bud  
245 proteomes. Contrary to proteome, metabolome allowed the classification of samples in relation to  
246 their ontogenetic age. This metabolomic differentiation was mainly caused by differences in  
247 photosynthesis, aminoacid synthesis and metabolism, redox regulation, and nucleotide  
248 metabolism.

249 These differences between mature and young buds and their basal and apical sections may be  
250 related to the location of the shoot apical meristem (SAM) activity in the apical section of the bud  
251 and also to the differential growth and developmental patterns of young and mature buds, as it  
252 was demonstrated by the differential accumulation of sample-specific pathways. Furthermore, the  
253 accumulation of a higher number of specific metabolites in comparison to proteins revealed the  
254 potential effect over the metabolome of the changes related to a smaller number of proteins.  
255 Alterations of key enzymes of metabolic pathways may lead to changes in abundance of a large  
256 number of metabolites. On the other hand, samples with a great ontogenic and functional  
257 differentiation (young vs mature) shared numerous proteins, which diffculted their classification  
258 according to their developmental stage. However, metabolites allowed their classification,  
259 reflecting the importance of metabolomic specificity in functional differentiation. The metabolome  
260 is the final downstream product of gene transcription and, therefore, changes in it are amplified  
261 relative to the changes in transcriptome and proteome (Das et al., 2015; Escandón et al., 2017).  
262 As young buds present more active development than differentiated mature buds, it is expected  
263 an overaccumulation of metabolites related to active processes of development, such as redox  
264 activity or aminoacid synthesis.

265

## 266 **The integrative analysis of proteome and metabolome unmasked potential** 267 **interaction networks involved in bud maturation and differentiation in *Pinus*** 268 ***pinaster***

269 The combination of different omic levels in an integrative analysis supposes a major analytical  
270 advantage since the different levels can be used for cross-validation and, at the same time, to get  
271 a global overview of the physiological processes (Singh et al., 2018). For this purpose, we

1  
2  
3 272 employed DIABLO algorithm (Rohart et al., 2017) to analyze proteome and metabolome datasets  
4 273 (Figure 3). This approach provided a better clustering of the samples at proteome and  
5 274 metabolome levels (Figure 3A). The joint analysis of both datasets correctly classified studied  
6 275 tissues (Figure 3B). The basis of this classification relied on the biological source of variation  
7 276 gathered by two main components, which collectively accounted 59% of the total variance  
8 277 (Supplementary Table S5). The analysis of the variables exhibiting highest loadings to these  
9 278 components (Figure 3C-D; Supplementary Table S5) allowed a biological interpretation of these  
10 279 results.

11 280 Component 1 gathered the variation related to ontogenic differentiation, distinguishing between  
12 281 young and mature buds. Enzymes related to energy, protein biosynthesis, lipid metabolism, and  
13 282 signaling/differentiation showed the highest correlations to this component (Figure 3C). Young  
14 283 tissues were characterized by an increased accumulation of energy-related ATPases or PSII  
15 284 reaction center proteins as well as several ribosomal- and RNA-related proteins. Lipids are  
16 285 supposed to be relevant players in this differentiation, and despite no differential lipids were  
17 286 identified after metabolome analysis, enzymes related to their metabolism were key nodes of our  
18 287 models. ACETYLCOA CARBOXYLASE CARBOXYL TRANSFERASE SUBUNIT ALPHA, which  
19 288 is a key lipidic enzyme as seen above (Harwood, 1996), a START-like domain, whose function in  
20 289 lipid regulation in plants was previously suggested (Ponting and Aravind, 1999), and GDSL  
21 290 ESTERASE LIPASE, being described its function in development, defense, synthesis of  
22 291 secondary metabolites, and morphogenesis in some plant species (Chepyshko et al., 2012), were  
23 292 some of the most highlighted lipidic-related enzymes.

24 293 On the other hand, RAS proteins, 14-3-3 transcription factors and DNA regulatory proteins by  
25 294 epigenetic mechanisms were re-emphasized as key processes in bud differentiation (Figure 3B).  
26 295 HISTONE 3 and HISTONE 4 (Tariq and Paszkowski, 2004; Valledor et al., 2010b; Bräutigam et  
27 296 al., 2013), GLYCOSYL HYDROLASES FAMILY 100 (Penterman et al., 2007), and RAS related  
28 297 proteins (Kamada et al., 1992; Alonso et al., 2007) regulate developmental processes, and were  
29 298 important to explain the ontogenic differences in the analyzed tissues. Many of these proteins  
30 299 were correlated to primary and secondary metabolites, some of which are characteristic of specific  
31 300 physiological stages, and therefore, having a potential involvement in development. Even though  
32 301 none of the most significant metabolites were identified in public databases, it would be interesting  
33 302 to highlight some of them due to their possible importance in differentiation interaction networks.  
34 303 Specifically, in ontogenic differentiation, significant metabolites (P0340, N1518, P0320, and  
35 304 N1292) seemed to differentiate young from mature buds (Figure 3D; Supplementary Table S5).

36 305 Second component distinguished between the apical and basal parts of the bud. Enzymes related  
37 306 to protein biosynthesis and folding-related, as well as peroxidases, were characteristic of this  
38 307 component (Figure 3C). Apical sections of the bud showed a positive correlation, and were  
39 308 characterized by increased abundance of stress-related proteins such as CHAPERONIN-LIKE  
40 309 TCP1 and others (Wang et al., 2004), a MANGANESE BINDING SITE from a GERMIN, which is  
41 310 related to abiotic and biotic stresses response in plants (Woo et al., 2000), and a PEROXIDASE.

1  
2  
3 311 On the other hand, key variables defining the basal parts of the buds showed negative correlation  
4 312 to this component. Basal sections were characterized by higher growth and proliferation rates  
5 313 than apical, fact that explains the importance of proteins related to cell division and reorganization  
6 314 such as PROFILIN 1 or PROHIBITIN 1 in this model. This last protein was only found in basal  
7 315 sections of mature bud, having multiple functions related to plant development and stress  
8 316 tolerance (Chen et al., 2005). In the same way, several transferases such as PYRIDOXAL  
9 317 PHOSPHATE DEPENDENT TRANSFERASE or PHOSPHORIBOSYLGLYCINAMIDE  
10 318 FORMYLTRANSFERASE were characteristic of the basal section of the bud. Most of the  
11 319 metabolites associated to this component were not identified. Among identified metabolites,  
12 320 loganin and deoxyloganin were only detected in apical sections of the bud, while basal had only  
13 321 highlighted unidentified metabolites (P1560 + P1340, N2243 and P1379) (Figure 3D;  
14 322 Supplementary Table S5).

15  
16  
17  
18  
19  
20  
21 323 The clustering and heatmap visualization of this integrative analysis (Figure 3B; Supplementary  
22 324 Figure S1) complemented results described above, revealing four different sets of variables:  
23 325 those proteins and metabolites over-accumulated in apical section of young bud and down-  
24 326 accumulated in the rest of the samples; those over-accumulated in basal section of young bud and  
25 327 down-accumulated in the rest of the samples; those over-accumulated in young buds and not in  
26 328 matures; and those over-accumulated in mature buds but not in young ones. First set of variables  
27 329 was mainly composed by metabolites and proteins already referenced such as GERMIN  
28 330 MANGANESE BINDING PROTEIN, PHOSPHOGLUCONATE DEHYDROGENASE or ribosomal  
29 331 proteins; conversely, second set of proteins was essentially constituted by proteins from different  
30 332 metabolic pathways such as photosynthesis, redox mechanism or signaling. Above all the  
31 333 differential variables found in the third set of proteins, this group was characterized by numerous  
32 334 proteins belonging on the one hand to stress pathways such as the previously described CPN10  
33 335 or H-TYPE THIOREDOXIN (Zhang et al., 2011) and EPOXIDE HYDROLASE (Morisseau, 2013)  
34 336 like proteins, and on the other hand, to energetic routes with a large number of proteins identified  
35 337 (ATP-DEPENDENT 6-PHOSPHOFRUCTOKINASE 2, MALATE DEHYDROGENASE,  
36 338 CYTOCHROME C, V-TYPE PROTON ATPase SUBUNIT D, SUCCINATE DEHYDROGENASE  
37 339 UBIQUINONE FLAVOPROTEIN SUBUNIT). Likewise, previously highlighted proteins related to  
38 340 lipid metabolism (ACETYL-COA ACETYLTRANSFERASE) and cellular reorganization  
39 341 (PROFILIN 1 and PROHIBITIN 1) were found in this pattern. Last set, including those proteins  
40 342 characteristic of mature buds, differentiation was established by a large number of non-identified  
41 343 metabolites and a small number of proteins, including ribosomal proteins, 14-3-3, HISTONE H3  
42 344 or GLYCOSYL HYDROLASE FAMILY 100 previously described.

43  
44  
45  
46  
47  
48  
49  
50  
51  
52  
53  
54 346 **The analysis of proteome-metabolome interaction combined with targeted**  
55 347 **transcriptomics allowed a deeper characterization of the bud**  
56 348 **differentiation process**  
57  
58  
59  
60

1  
2  
3 349 The integration of metabolome and proteome datasets also allowed the definition of a protein-  
4 350 metabolite interaction network based on the different correlations between variables of different  
5 351 types. The resulting network (Figure 4; correlation >0.75) showed two interaction clusters. First  
6 352 cluster (Figure 4A, left) gathered proteins and metabolites more abundant in the apical sections  
7 353 of young buds (Figures 4B-D). Proteins in this cluster are related to protein biosynthesis and  
8 354 transport (ribosomal-related, CHAPERONIN TCP1, TMP21), transcriptional response to stress  
9 355 (GERMIN, NUCLEIC ACID BINDING PROTEIN), and a PHOSPHOESTERASE similar to  
10 356 Arabidopsis PURPLE ACID PHOSPHATASE, PAP14 (At2g46880), required for petal  
11 357 differentiation and expansion (Zhu et al., 2005). These proteins positively correlated to different  
12 358 terpenoids (mascaroside, loganin, menthane) and the flavonoid luteolin. The abundance of these  
13 359 variables greatly diminished during the transition to basal section and also in mature buds. 4,4'-  
14 360 ditolylthiourea, the only metabolite in this cluster whose abundance is maximal in the basal section  
15 361 of mature buds, showed negative correlations to all of its linked nodes.

16 362 Second cluster (Figure 4A, right) was not as selective in its variable categories as first cluster,  
17 363 since groups variables peaking at each developmental stage and bud section. However, there  
18 364 was a major presence of variables more accumulated in mature tissues and/or basal sections of  
19 365 the buds (Figures 4C, D). Young buds are characterized by an increased photosynthesis (active  
20 366 center of PSII, GAPDH) and glycolytic (PYRUVATE KINASE, PHOSPHOFRUCTOKINASE)  
21 367 pathways. HISTONE H4, GDSL ESTERASE LIPASE, and elements related to protein  
22 368 biosynthesis (eRF1, protease inhibitor SERPIN, ribosomal proteins L15 and L50) and redox  
23 369 (THIOREDOXIN, START-like domain protein) were also more abundant in young buds. Most of  
24 370 these enzymes were positively correlated to N1751, an unknown metabolite, and were  
25 371 characteristic of basal sections of the bud. On the other hand, mature buds had increased  
26 372 energetic (fructose-6-P and ATPase), signaling and gene regulation (14-3-3 protein gamma,  
27 373 HISTONE H3, regulator of ribonuclease activity), antioxidant/detoxification activities  
28 374 (dihydrolipoate), and proteome remodeling (ribosomal proteins and peptidases). 2-alpha-(S)-  
29 375 Strictosidine, a key compound in monoterpene indol alkaloyds biosynthetic pathway (Rüffer et al.,  
30 376 1978), was mostly accumulated in the basal sections.

31 377 Interestingly, HISTONE H3, and other proteins related to epigenetic regulation of gene expression  
32 378 formed a cluster that had a greater accumulation in mature buds. Despite having a positive  
33 379 correlation to most of the metabolites of this cluster, it negatively correlated to those metabolites  
34 380 accumulated in young buds. HISTONE H4, characteristic of young tissues, negatively correlated  
35 381 to metabolite P0265 and through it to glycolytic and carbon-related enzymes, suggesting its role  
36 382 in regulation of energetic pathways. Finally, 14-3-3 Protein gamma, involved in the signaling  
37 383 pathways of the main plant hormones (Camoni et al., 2018), was also accumulated in mature  
38 384 buds in the apical section. However, in this case, it was negatively correlated to most of the  
39 385 metabolites in this cluster, some of them as relevant as diphyllin, lignin (Hemmati et al., 2007), or  
40 386 fructose-6-P.

387 In order to support hypotheses raised after proteometabolomic dataset, six genes related to the  
388 different activities of the clusters depicted above were analyzed by qPCR (Figure 5). According  
389 to transcriptomics results, the different treatment had different expression patterns of the analyzed  
390 genes. Apical section of young buds had a differential overexpression of  
391 *ADENOSYLHOMOCYSTEINASE (SAHH)*, related to epigenetic regulation (Tanaka et al., 1997;  
392 Rocha et al., 2005), and *GLUTATHIONE S-TRANSFERASE (GST)* and *PHENYLALANINE*  
393 *AMMONIA LYASE (PAL)*, both genes involved in secondary metabolism and hormonal signaling  
394 (Hahlbrock and Scheel, 1989; Rivero et al., 2001; Dixon et al., 2010; Czerniawski and Bednarek,  
395 2018). The expression level of these genes was similar in mature buds and in the basal part of  
396 the young bud.

397 *S-ADENOSYLMETHIONINE SYNTHASE (SAM SYNTHASE)*, a central element in DNA  
398 methylation (Gómez-Gómez and Carrasco, 1998) was more expressed in young buds, as  
399 *NEDD8-ACTIVATING ENZYME E1 CATALYTIC SUBUNIT (NEDD8-E1)*, involved in proteome  
400 remodelling and DNA repair (Brown and Jackson, 2015; Brown et al., 2015). Finally, it is important  
401 to highlight the expression pattern of the *MORE AXILLARY GROWTH 1 (MAX1)* gene, which is  
402 required for hormonal biosynthesis of a shoot-branching inhibiting signal (Booker et al., 2005).  
403 *MAX1* increased its expression in young basal section, while its expression decreased drastically  
404 in mature basal section.

405

## 406 **DISCUSSION**

407 The study of the transition between young and mature buds, and how it is reflected at metabolome  
408 and proteome levels, is not only crucial in order to understand shoot growth and tree architecture,  
409 but also to improve relevant traits for forestry such as total growth or polycyclism (Cabezas et al.,  
410 2015). Growth-related traits are influenced not only by their inherent genetic factors (most of them  
411 polygenic) but also by the environment (Zas and Fernández-López, 2005). Environmental  
412 conditions (light, temperature, rainfall) in combination with the genotype define not only the yearly  
413 tree growth period, ontogenic stage and flowering time, but also tree architecture, modulating for  
414 instance, polycyclism (Meijón et al., 2016; de Simón et al., 2018). The combination of genetic and  
415 environmental factors, together with the different growth patterns of mature and young buds  
416 sometimes mixed in trees of the same age, makes the apical growth in *Pinus pinaster* very  
417 complex at physiological and molecular levels (Nguyen et al., 1995). Consequently, the  
418 characterization of the proteome and metabolome of buds in different developmental stages is a  
419 necessary first step towards the fully understanding of all of these processes.

420 The employment of an integrative approach allowed the characterization of bud maturation from  
421 a holistic perspective, identifying the key molecular pathways of this process. Two main sources  
422 of variation were clearly distinguished after clustering and multivariate analyses. The first was the  
423 bud maturation status (young vs mature) and the second the presence of apical or lateral  
424 meristems (apical vs basal section of the buds), each of them with a different set of characteristic  
425 biomolecules.

1  
2  
3 426 Mature buds exhibit specific phenology and growth patterns distinct from young buds. In the  
4 427 young stage, leaf primordia differentiate into photosynthetically active primary needles. Axillary  
5 428 buds develop either into auxiblasts in basal positions or into randomly distributed brachyblasts in  
6 429 more distal positions on the stem. When trees reach the mature stage, leaf primordia differentiate  
7 430 into scale leaves, and photosynthetic activity is shifted to long needles differentiated on  
8 431 brachyblasts (Nguyen et al., 1995; Jordy, 2004). The physiological competence of mature buds  
9 432 was probably imposed by the increased abundance of ABA and specific gibberelins (bioactive  
10 433 GA1 and intermediary GA19; Supplementary Table S3). ABA has not only a role in dormancy,  
11 434 but also in dormancy release and bud set in combination with specific gibberellins (Zheng et al.,  
12 435 2015; Maurya et al., 2018; Vimont et al., 2019). Interestingly, young buds had slightly lower  
13 436 concentrations of ABA but an increased abundance of bioactive GA3, and GA8, a degradation  
14 437 product of GA1. Both gibberellins, GA1 and GA3, are related to shoot elongation (Little and  
15 438 MacDonald, 2003); however, is complicated to venture which specific role are playing each one  
16 439 in the different development stage of the bud. Additionally, in relation to hormonal signaling, a key  
17 440 element was identified in the network, 14-3-3 protein. A possible role for 14-3-3 proteins in the  
18 441 coordination of GA and ABA signaling has emerged in the last years (Camoni et al., 2018). In  
19 442 fact, the overexpression of ABA responsive, 14-3-3-interacting transcription factors ABF1-3  
20 443 impairs GA action, indicating that they act as negative regulators of GA signaling and that 14-3-3  
21 444 proteins may function by sequestering ABF1-3 in the cytoplasm. However, the mechanism of 14-  
22 445 3-3 action and all the elements involved in the ABA and GA coordination are still unknown.

23 446 As pointed by datasets and correlation networks, having the enzymatic machinery to increase  
24 447 metabolic rate allowing burst and growth seems to be essential in young buds, since enzymes of  
25 448 photosynthesis and glycolytic pathways were increased compared to mature (Figures 2 and 4).  
26 449 Interestingly, the accumulation of fructose-6-P in mature buds indicate not only a differential  
27 450 allocation of sugars between ontogenic stages, but also specific hormonal, growth (Eveland and  
28 451 Jackson, 2012), and maturation patterns (Uggla et al., 2001). Lipids such as pimelate and  
29 452 dihydroxylopoate with a dual redox and transcriptional regulation role (Sen and Packer, 1996)  
30 453 were also accumulated in mature buds. The mature secondary metabolism was also reflected by  
31 454 the accumulation of flavonoids. Flavonoids and tannins may be involved in cellular detoxification  
32 455 (Meijón et al., 2016) and also in plant resistance against herbivores or other stresses (Treutter,  
33 456 2008). At the end of the growing season, accumulation of lipid and starch is positively correlated  
34 457 with the onset of dormancy in mature buds (Jordy, 2004). Bud development is also associated to  
35 458 different abiotic stress tolerance and proteins related to detoxification. In all analyzed tissues,  
36 459 there were a great abundance of heat shock or chaperonin-like proteins (TCP1, CPN10) and ROS  
37 460 detoxifying enzymes (peroxidases, thioredoxines); however, mature buds were characterized by  
38 461 higher abundances of these protein families, suggesting that the greater tolerance to stress  
39 462 exhibited by these buds (Miller et al., 2008) relies on the overaccumulation of these molecules,  
40 463 compared to young tissues.

41 464 The different cell competence is defined by specific protein sets consequence of differential  
42 465 transcriptional and post-transcriptional regulation (del Mar Castellano et al., 2004; Dembinsky et

1  
2  
3 466 al., 2007). Mature and young buds have a differential set of DNA/RNA interacting proteins and  
4 467 ribosomal proteins. Among them, START-like domain proteins were up-accumulated in young  
5 468 tissues, despite one characteristic of mature buds (PPI00057470). The specific dynamic of this  
6 469 family, which is required for regulating transcription factors needed for cell differentiation after  
7 470 binding a lipid ligand (Schrick et al., 2014; Grabon et al., 2019), illustrates the complexity of bud  
8 471 maturation. Young buds were characterized by the serin protease inhibitors SERPIN (+5-fold  
9 472 change compared to mature) (Supplementary Table S2), which has been proposed to have also  
10 473 a non-peptidase inhibitory functions negatively regulating stress-induced cell death or reducing  
11 474 gene expression by compacting chromatin (Cohen et al., 2019). Epigenetic regulation elements  
12 475 were also differential between mature and young buds (discussed below).

13  
14  
15  
16  
17  
18 476 The complexity of a pine bud was also reflected in the direct comparison of its apical and basal  
19 477 sections. The former containing the shoot apical meristem, and the later the lateral meristems  
20 478 and needle primordia (Fernando, 2014). This organization implies physiological and metabolic  
21 479 differences, which has been validated through this work. Starch, lipid reserves, and tannins are  
22 480 known to accumulate in the shoot tip as pines become older (Jordy et al., 2000; Jordy, 2004). The  
23 481 accumulation of flavonoids and its biosynthetic machinery in the apical part of the buds reinforces  
24 482 its role in the protection of the meristem (Meijón et al., 2016) and also in the vegetative bud  
25 483 outgrowth. Differential organogenetic activity in apical and basal sections, changeable across the  
26 484 bud maturation, is also related to environment conditions and apical dominance regulation (Jordy,  
27 485 2004; Hover et al., 2017). Thus, the high activity of *MAX1* gene in both sections of young bud  
28 486 suggests the essential role of strigolactone hormone regulating inhibition of axillary bud outgrowth  
29 487 in this phase; however, in mature bud, *MAX1* expression is higher in apical section (Figure 5).  
30 488 The current models in relation to control of apical dominance suggest complex interaction  
31 489 networks where sugars and ABA could be responsible for initial release of an apical bud, while  
32 490 auxins, strigolactones and cytokinins seem to determine sustained outgrowth of axillary buds  
33 491 (Nguyen and Emery, 2017). Gibberellins, despite being their role well known in shoot elongation,  
34 492 need more investigation to determine their function inside this network. However, some reports  
35 493 on their interaction with strigolactone suggest that increased gibberellin levels could repress  
36 494 axillary bud outgrowth (Luisi et al., 2011).

37  
38  
39  
40  
41  
42  
43  
44  
45 495 The basal part of the bud is prepared to burst, contrary to apical whose function is keeping and  
46 496 protecting apical meristem, and many cell division and development-related proteins like FTSZ  
47 497 needed for plastid division (Schmitz et al., 2009), dormancy/associated or DNA repair machinery  
48 498 (Os08g0519400 like protein) were up-accumulated. LEA proteins and TMP21, associated to less  
49 499 differentiated organs (Zimmerman, 1993), were characteristic of the apical part of the buds  
50 500 probably helping to maintain meristem identity together with specific abundances of growth  
51 501 regulators and nucleic acid binding proteins and histone modifications regulating gene  
52 502 expression.

53  
54  
55  
56  
57  
58 503 The great amount of differential proteins and metabolites involved in epigenetic regulation  
59 504 suggests the key role of these mechanisms in bud development. DNA methylation is a well-known  
60

1  
2  
3 505 epigenetic mark of transcriptional gene silencing, but also in the establishment of  
4 506 heterochromatin, transposon control and genomic imprinting (Galindo-González et al., 2018).  
5  
6 507 Two of the key enzymes regulating the methylation cycle, SAM SYNTHASE and SAHH, showed  
7  
8 508 an overaccumulation in young buds and more specifically in its apical part (Figure 5), suggesting  
9  
10 509 that bud maturation is concomitant to increased DNA methylation levels as previously reported in  
11  
12 510 *Pinus radiata* (Fraga et al., 2002). ARGONAUTE, a key enzyme involved in RNA-mediated DNA  
13  
14 511 methylation, was overaccumulated in mature apical buds, which will be probably related to the  
15  
16 512 hypermethylation associated to development. Despite the employed analytical procedures were  
17  
18 513 not intended to describe post-translational modifications defining histone code, specific forms of  
19  
20 514 HISTONE H3 and H4 were characteristic of each developmental stage, reinforcing the hypothesis  
21  
22 515 that bud maturation is the consequence of a complex interaction between epigenetic  
23  
24 516 mechanisms, transcription factors and hormonal regulators.

25  
26 517 Overall, our study provided novel insights over bud maturation and the machinery involved in its  
27  
28 518 development and growth and stress resilience at different molecular levels and pathways. The  
29  
30 519 comprehensive overview of this process allowed the validation of proteins and metabolites  
31  
32 520 involved in bud development that were previously described, but also the involvement of novel  
33  
34 521 proteins, metabolites, and pathways. However, further studies will be necessary to validate these  
35  
36 522 new set of candidate molecules by using buds coming from different populations that show  
37  
38 523 contrasting wood quality and stress tolerance.

39 524

## 40 525 **DATA AND MATERIALS AVAILABILITY**

41 526 All relevant data can be found within the manuscript and supplementary materials.

42 527

## 43 528 **SUPPLEMENTARY MATERIAL**

44 529 **Table S1.** Genes and primers employed in quantitative PCR analyses.

45 530 **Table S2.** Proteins identification according to SEQUEST (scores, % of coverage, number of  
46 531 common, unique, and razor peptides), quantification (mean  $\pm$  SD of three biological replicates),  
47 532 univariate analysis (p and q values; TukeyHSD p values for all paired comparisons).

48 533 **Table S3.** Peaks obtained after UPLC-MS analysis of polar metabolites. Peaks were aligned with  
49 534 mzMine 2.10 avoiding redundancies between positive (P) and negative (N) modes. This table  
50 535 shows peak ID, adduct, m/z, retention time, normalized peak areas for each analyzed sample,  
51 536 and univariate analysis (p and q values; TukeyHSD p values for all paired comparisons). Peak  
52 537 compound description is provided according to Supplementary Table S4.

53 538 **Table S4.** Identification of metabolites in the 3670 peaks that were analyzed. a) 133 peaks were  
54 539 unequivocally identified (those metabolites that were defined after the comparison to our  
55 540 compound library or by comparison of the MS/MS to *online* databases). b) 987 peaks were  
56 541 tentatively assigned after comparing its very accurate mass to reference compound databases.  
57 542 Delta ppm and compound exact mass are provided. Annotation source, molecular form, and



1  
2  
3 543 accessions of KEGG, FooDB and other databases are provided for all identified/assigned  
4 544 compounds.

5 545 **Table S5.** DIABLO integrative analysis of proteome and metabolome datasets. a) Sample scores  
6 546 for components 1 and 2 in both datasets, b) variance explained for each component, and c)  
7 547 variable loadings for both datasets.

8 548 **Figure S1.** Integrative clustering of proteome and metabolome analysis (High resolution Figure  
9 549 3B).

10 550

## 11 551 **DISCLOSURES**

12 552 The authors have no conflicts of interest to declare.

13 553

## 14 554 **FUNDING**

15 555 This publication is an output of the National Project Vampiro (AGL2017-83988-R, Spanish  
16 556 Ministry of Economy and Competitiveness). M.M. and L.V. were supported by Ramón y Cajal  
17 557 program (RYC-2014-14981 and RYC-2015-17871, respectively; Spanish Ministry of Economy  
18 558 and Competitiveness). L.G.C and S.G. were supported by Severo Ochoa Predoctoral Program  
19 559 (BP19-146 and BP19-145, respectively; Principality of Asturias, Spain).

20 560

## 21 561 **ACKNOWLEDGMENTS**

22 562 The authors wish to thank Eloy A. Ron (SERPA S.A, Vivero Forestal de La Mata) for providing  
23 563 the *Pinus pinaster* seedlings employed in this work.

24 564

## 25 565 **AUTHORS' CONTRIBUTIONS**

26 566 MM and LV designed the experiments, performed mass-spectrometry analyses, and  
27 567 metabolome-related computational analysis. LV and SG performed proteome-related  
28 568 computational analysis. LGC performed targeted-transcriptomics analyses. LV and SG performed  
29 569 statistical analyses. All authors wrote the manuscript, read, and approved the final version of the  
30 570 manuscript.

31 571  
32  
33  
34  
35  
36  
37  
38  
39  
40  
41  
42  
43  
44  
45  
46  
47  
48  
49  
50  
51  
52  
53  
54  
55  
56  
57  
58  
59  
60

572

## REFERENCES

574

575 Allenbach, L., and Poirier, Y. (2000). Analysis of the alternative pathways for the  $\beta$ -oxidation of  
 576 unsaturated fatty acids using transgenic plants synthesizing polyhydroxyalkanoates in  
 577 peroxisomes. *Plant Physiol.* 124, 1159-1168. doi: 10.1104/pp.124.3.1159

578 Allona, I., Quinn, M., Shoop, E., Swope, K., Cyr, S.S., Carlis, J., et al. (1998). Analysis of xylem  
 579 formation in pine by cDNA sequencing. *Proc. Natl. Acad. Sci. U.S.A.* 95, 9693-9698. doi:  
 580 10.1073/pnas.95.16.9693

581 Alonso, P., Cortizo, M., Cantón, F.R., Fernández, B., Rodríguez, A., Centeno, M.L., et al. (2007).  
 582 Identification of genes differentially expressed during adventitious shoot induction in  
 583 *Pinus pinea* cotyledons by subtractive hybridization and quantitative PCR. *Tree Physiol.*  
 584 27, 1721-1730. doi: 10.1093/treephys/27.12.1721

585 Baldermann, S., Homann, T., Neugart, S., Chmielewski, F.-M., Götz, K.-P., Gödeke, K., et al.  
 586 (2018). Selected plant metabolites involved in oxidation-reduction processes during bud  
 587 dormancy and ontogenetic development in sweet cherry buds (*Prunus avium* L.).  
 588 *Molecules* 23, 1197. doi: 10.3390/molecules23051197

589 Booker, J., Sieberer, T., Wright, W., Williamson, L., Willett, B., Stirnberg, P., et al. (2005). *MAX1*  
 590 encodes a cytochrome P450 family member that acts downstream of *MAX3/4* to produce  
 591 a carotenoid-derived branch-inhibiting hormone. *Dev. Cell.* 8, 443-449. doi:  
 592 10.1016/j.devcel.2005.01.009

593 Bräutigam, K., Vining, K.J., Lafon-Placette, C., Fossdal, C.G., Mirouze, M., Marcos, J.G., et al.  
 594 (2013). Epigenetic regulation of adaptive responses of forest tree species to the  
 595 environment. *Ecol. Evol.* 3, 399-415. doi: 10.1002/ece3.461

596 Brown, J.S., and Jackson, S.P. (2015). Ubiquitylation, neddylation and the DNA damage  
 597 response. *Open Biol.* 5, 150018. doi: 10.1098/rsob.150018

598 Brown, J.S., Lukashchuk, N., Sczaniecka-Clift, M., Britton, S., le Sage, C., Calsou, P., et al.  
 599 (2015). Neddylation promotes ubiquitylation and release of Ku from DNA-damage sites.  
 600 *Cell Rep.* 11, 704-714. doi: 10.1016/j.celrep.2015.03.058

601 Brunner, A.M., Varkonyi-Gasic, E., and Jones, R.C. (2017). "Phase change and phenology in  
 602 trees," in *Comparative and evolutionary genomics of angiosperm trees*, eds A. T. Groover  
 603 and Q. C. B. Cronk (Cham: Springer International Publishing AG), 227-274.

604 Byrne, M.E. (2009). A role for the ribosome in development. *Trends Plant Sci.* 14, 512-519. doi:  
 605 10.1016/j.tplants.2009.06.009

606 Cabezas, J.A., González-Martínez, S.C., Collada, C., Guevara, M.A., Boury, C., de María, N., et  
 607 al. (2015). Nucleotide polymorphisms in a pine ortholog of the Arabidopsis degrading  
 608 enzyme cellulase KORRIGAN are associated with early growth performance in *Pinus*  
 609 *pinaster*. *Tree Physiol.* 35, 1000-1006. doi: 10.1093/treephys/tpv050

610 Camoni, L., Visconti, S., Aducci, P., and Marra, M. (2018). 14-3-3 proteins in plant hormone  
 611 signaling: doing several things at once. *Front. Plant Sci.* 9, 297. doi:  
 612 10.3389/fpls.2018.00297

613 Canales, J., Bautista, R., Label, P., Gómez-Maldonado, J., Lesur, I., Fernández-Pozo, N., et al.  
 614 (2014). De novo assembly of maritime pine transcriptome: implications for forest breeding  
 615 and biotechnology. *Plant Biotechnol. J.* 12, 286-299. doi: 10.1111/pbi.12136

616 Cano, M., Morcillo, A., Humánez, A., Mendoza-Poudereux, I., Alborch, A., Segura, J., et al.  
 617 (2018). "Maritime Pine (*Pinus Pinaster* Aiton)," in *Step Wise Protocols for Somatic*  
 618 *Embryogenesis of Important Woody Plants: Volume I Forestry Sciences 84*, eds S. M.  
 619 Jain and P. Gupta (Cham: Springer International Publishing AG), 167-179.

620 Cañas, R.A., Canales, J., Muñoz-Hernández, C., Granados, J.M., Ávila, C., García-Martín, M.L.,  
 621 et al. (2015). Understanding developmental and adaptive cues in pine through metabolite  
 622 profiling and co-expression network analysis. *J. Exp. Bot.* 66, 3113-3127. doi:  
 623 10.1093/jxb/erv118

624 Chen, J.C., Jiang, C.Z., and Reid, M.S. (2005). Silencing a prohibitin alters plant development  
 625 and senescence. *Plant J.* 44, 16-24. doi: 10.1111/j.1365-313X.2005.02505.x

626 Chepyshko, H., Lai, C.-P., Huang, L.-M., Liu, J.-H., and Shaw, J.-F. (2012). Multifunctionality and  
 627 diversity of GDSL esterase/lipase gene family in rice (*Oryza sativa* L. *japonica*) genome:  
 628 new insights from bioinformatics analysis. *BMC Genomics.* 13, 309. doi: 10.1186/1471-  
 629 2164-13-309

- 1  
2  
3 630 Cohen, M., Davydov, O., and Fluhr, R. (2019). Plant serpin protease inhibitors: specificity and  
4 631 duality of function. *J. Exp. Bot.* 70, 2077-2085. doi: 10.1093/jxb/ery460
- 5 632 Conde, D., Moreno-Cortés, A., Dervinis, C., Ramos-Sánchez, J.M., Kirst, M., Perales, M., et al.  
6 633 (2017). Overexpression of DEMETER, a DNA demethylase, promotes early apical bud  
7 634 maturation in poplar. *Plant Cell Environ.* 40, 2806-2819. doi: 10.1111/pce.13056
- 8 635 Czerniawski, P., and Bednarek, P. (2018). Glutathione S-transferases in the biosynthesis of  
9 636 sulfur-containing secondary metabolites in Brassicaceae plants. *Front. Plant Sci.* 9, 1639.  
10 637 doi: 10.3389/fpls.2018.01639
- 11 638 Das, A., Paudel, B., and Rohila, J.S. (2015). "Potentials of proteomics in crop breeding," in  
12 639 *Advances in plant breeding strategies: breeding, biotechnology and molecular tools*, eds  
13 640 J. M. Al-Khayri, S. M. Jain and D. V. Johnson (Cham: Springer International Publishing  
14 641 AG), 513-537.
- 15 642 De Simón, B.F., Cadahía, E., and Aranda, I. (2018). Metabolic response to elevated CO<sub>2</sub> levels  
16 643 in *Pinus pinaster* Aiton needles in an ontogenetic and genotypic-dependent way. *Plant*  
17 644 *Physiol. Biochem.* 132, 202-212. doi: 10.1016/j.plaphy.2018.09.006
- 18 645 De Simón, B.F., Sanz, M., Cervera, M.T., Pinto, E., Aranda, I., and Cadahía, E. (2017). Leaf  
19 646 metabolic response to water deficit in *Pinus pinaster* Ait. relies upon ontogeny and  
20 647 genotype. *Environ. Exp. Bot.* 140, 41-55. doi: 10.1016/j.envexpbot.2017.05.017
- 21 648 Del Mar Castellano, M., Boniotti, M.B., Caro, E., Schnittger, A., and Gutierrez, C. (2004). DNA  
22 649 replication licensing affects cell proliferation or endoreplication in a cell type-specific  
23 650 manner. *Plant Cell* 16, 2380-2393. doi: 10.1105/tpc.104.022400
- 24 651 Dembinsky, D., Woll, K., Saleem, M., Liu, Y., Fu, Y., Borsuk, L.A., et al. (2007). Transcriptomic  
25 652 and proteomic analyses of pericycle cells of the maize primary root. *Plant Physiol.* 145,  
26 653 575-588. doi: 10.1104/pp.107.106203
- 27 654 Dixon, D.P., Skipsey, M., and Edwards, R. (2010). Roles for glutathione transferases in plant  
28 655 secondary metabolism. *Phytochemistry* 71, 338-350. doi:  
29 656 10.1016/j.phytochem.2009.12.012
- 30 657 Escandón, M., Valledor, L., Pascual, J., Pinto, G., Cañal, M.J., and Meijón, M. (2017). System-  
31 658 wide analysis of short-term response to high temperature in *Pinus radiata*. *J. Exp. Bot.*  
32 659 68, 3629-3641. doi: 10.1093/jxb/erx198
- 33 660 Eveland, A.L., and Jackson, D.P. (2012). Sugars, signalling, and plant development. *J. Exp. Bot.*  
34 661 63, 3367-3377. doi: 10.1093/jxb/err379
- 35 662 FAO (2009). *Global demand for wood products. Rome: Italy: The Food and Agricultural*  
36 663 *Organization of the United Nations.* Available at:  
37 664 <http://www.fao.org/3/i0350e/i0350e00.htm>
- 38 665 FAO (2015). *Global forest resources assessment 2015. Rome, Italy.* FAO Forestry Paper No. 1.  
39 666 Available at: [http://www.fao.org/forest-resources-assessment/past-assessments/fra-](http://www.fao.org/forest-resources-assessment/past-assessments/fra-2015/en/)  
40 667 [2015/en/](http://www.fao.org/forest-resources-assessment/past-assessments/fra-2015/en/)
- 41 668 Fernández, H., Fraga, M., Bernard, P., and Revilla, M. (2003). Quantification of GA1, GA3, GA4,  
42 669 GA7, GA9, and GA20 in vegetative and male cone buds from juvenile and mature trees  
43 670 of *Pinus radiata*. *Plant Growth Regul.* 40, 185-188. doi: 10.1023/A:1025070707899
- 44 671 Fernando, D.D. (2014). The pine reproductive process in temperate and tropical regions. *New*  
45 672 *For.* 45, 333-352. doi: 10.1007/s11056-013-9403-7
- 46 673 Fraga, M.F., Rodríguez, R., and Cañal, M.J. (2002). Genomic DNA methylation-demethylation  
47 674 during aging and reinvigoration of *Pinus radiata*. *Tree Physiol.* 22, 813-816. doi:  
48 675 10.1093/treephys/22.11.813
- 49 676 Galindo-González, L., Sarmiento, F., and Quimbaya, M.A. (2018). Shaping plant adaptability,  
50 677 genome structure and gene expression through transposable element epigenetic control:  
51 678 Focus on methylation. *Agronomy* 8, 180. doi: 10.3390/agronomy8090180
- 52 679 Garcés, M., Le Provost, G., Lalanne, C., Claverol, S., Barré, A., Plomion, C., et al. (2014).  
53 680 Proteomic analysis during ontogenesis of secondary xylem in maritime pine. *Tree*  
54 681 *Physiol.* 34, 1263-1277. doi: 10.1093/treephys/tp117
- 55 682 Girard, F., Vennetier, M., Ouarmim, S., Caraglio, Y., and Misson, L. (2011). Polycyclism, a  
56 683 fundamental tree growth process, decline with recent climate change: the example of  
57 684 *Pinus halepensis* Mill. in Mediterranean France. *Trees Struct. Funct.* 25, 311-322. doi:  
58 685 10.1007/s00468-010-0507-9
- 59 686 Gómez-Gómez, L., and Carrasco, P. (1998). Differential expression of the S-Adenosyl-L-  
60 687 Methionine Synthase genes during pea development. *Plant Physiol.* 117, 397-405. doi:  
61 688 10.1104/pp.117.2.397

1  
2  
3  
4  
5  
6  
7  
8  
9  
10  
11  
12  
13  
14  
15  
16  
17  
18  
19  
20  
21  
22  
23  
24  
25  
26  
27  
28  
29  
30  
31  
32  
33  
34  
35  
36  
37  
38  
39  
40  
41  
42  
43  
44  
45  
46  
47  
48  
49  
50  
51  
52  
53  
54  
55  
56  
57  
58  
59  
60

- 689 González, Á.C., Díaz, I.F., de la Torre, C., Vázquez, J.P., Colina, F.J., Valledor, L., et al. (2016).  
690 Nuevos marcadores de calidad de madera en *Pinus pinaster*: Estrigolactonas y  
691 ramificación. *Tecnología agroalimentaria: Boletín informativo del SERIDA* 17, 21-27.
- 692 Grabon, A., Bankaitis, V.A., and McDermott, M.I. (2019). The interface between  
693 phosphatidylinositol transfer protein function and phosphoinositide signaling in higher  
694 eukaryotes. *J. Lipid Res.* 60, 242-268. doi: 10.1194/jlr.R089730
- 695 Großskinsky, D.K., Syaifullah, S.J., and Roitsch, T. (2017). Integration of multi-omics techniques  
696 and physiological phenotyping within a holistic phenomics approach to study senescence  
697 in model and crop plants. *J. Exp. Bot.* 69, 825-844. doi: 10.1093/jxb/erx333
- 698 Haffner, V., Enjalric, F., Lardet, L., and Carron, M. (1991). Maturation of woody plants: a review  
699 of metabolic and genomic aspects. *Ann. For. Sci.* 48, 615-630. doi:  
700 10.1051/forest:19910601
- 701 Hahlbrock, K., and Scheel, D. (1989). Physiology and molecular biology of phenylpropanoid  
702 metabolism. *Annu. Rev. Plant Biol. Plant. Mol. Biol.* 40, 347-369. doi:  
703 10.1146/annurev.pp.40.060189.002023
- 704 Harwood, J.L. (1996). Recent advances in the biosynthesis of plant fatty acids. *Biochim. Biophys.*  
705 *Acta* 1301, 7-56. doi: 10.1016/0005-2760(95)00242-1
- 706 Hemmati, S., Schneider, B., Schmidt, T.J., Federolf, K., Alfermann, A.W., and Fuss, E. (2007).  
707 Justicidin B 7-hydroxylase, a cytochrome P450 monooxygenase from cell cultures of  
708 *Linum perenne* Himmelszelt involved in the biosynthesis of diphyllin. *Phytochemistry* 68,  
709 2736-2743. doi: 10.1016/j.phytochem.2007.10.025
- 710 Hover, A., Buissart, F., Caraglio, Y., Heinz, C., Pailler, F., Ramel, M., et al. (2017). Growth  
711 phenology in *Pinus halepensis* Mill.: apical shoot bud content and shoot elongation. *Ann.*  
712 *For. Sci.* 74, 39. doi: 10.1007/s13595-017-0637-y
- 713 Considine, M.J., and Foyer, C.H. (2014). Redox Regulation of Plant Development. *Antioxid.*  
714 *Redox Signal.* 21, 1305-1326. doi: 10.1089/ars.2013.5665
- 715 Jordy, M.-N., Danti, S., Favre, J.-M., and Raccchi, M.L. (2000). Histological and biochemical  
716 changes in *Pinus* spp. seeds during germination and post-germinative growth:  
717 triacylglycerol distribution and catalase activity. *Aust. J. Plant Physiol.* 27, 1109-1117. doi:  
718 10.1071/PP00069
- 719 Jordy, M.N. (2004). Seasonal variation of organogenetic activity and reserves allocation in the  
720 shoot apex of *Pinus pinaster* Ait. *Ann. Bot.* 93, 25-37. doi: 10.1093/aob/mch005
- 721 Kamada, I., Yamauchi, S., Youssefian, S., and Sano, H. (1992). Transgenic tobacco plants  
722 expressing *rgp1*, a gene encoding a RAS-related GTP-binding protein from rice, show  
723 distinct morphological characteristics. *Plant J.* 2, 799-807. doi: 10.1111/j.1365-  
724 313X.1992.tb00149.x
- 725 Kim, D., Shin, H., Song, Y.S., and Kim, J.H. (2012). Synergistic effect of different levels of genomic  
726 data for cancer clinical outcome prediction. *J. Biomed. Inform.* 45, 1191-1198. doi:  
727 10.1016/j.jbi.2012.07.008
- 728 Little, C., and MacDonald, J.E. (2003). Effects of exogenous gibberellin and auxin on shoot  
729 elongation and vegetative bud development in seedlings of *Pinus sylvestris* and *Picea*  
730 *glauca*. *Tree Physiol.* 23, 73-83. doi: 10.1093/treephys/23.2.73
- 731 Lohse, M., Nagel, A., Herter, T., May, P., Schroda, M., Zrenner, R., et al. (2014). Mercator: a fast  
732 and simple web server for genome scale functional annotation of plant sequence data.  
733 *Plant Cell Environ.* 37, 1250-1258. doi: 10.1111/pce.12231
- 734 López-Goldar, X., Villari, C., Bonello, P., Borg-Karlson, A.K., Grivet, D., Sampedro, L., et al.  
735 (2019). Genetic variation in the constitutive defensive metabolome and its inducibility are  
736 geographically structured and largely determined by demographic processes in maritime  
737 pine. *J. Ecol.* 107, 2464-2477. doi: 10.1111/1365-2745.13159
- 738 López-Goldar, X., Zas, R., Sampedro, L. (2020). Resource availability drives microevolutionary  
739 patterns of plant defences. *Funct. Ecol.*, 1-13. doi: 10.1111/1365-2435.13610
- 740 Luisi, A., Lorenzi, R., and Sorce, C. (2011). Strigolactone may interact with gibberellin to control  
741 apical dominance in pea (*Pisum sativum*). *Plant Growth Regul.* 65, 415-419. doi:  
742 10.1007/s10725-011-9603-0
- 743 Maurya, J.P., Triozzi, P.M., Bhalerao, R.P., and Perales, M. (2018). Environmentally sensitive  
744 molecular switches drive poplar phenology. *Front. Plant Sci.* 9, 1873. doi:  
745 10.3389/fpls.2018.01873
- 746 Meijón, M., Feito, I., Oravec, M., Delatorre, C., Weckwerth, W., Majada, J., et al. (2016). Exploring  
747 natural variation of *Pinus pinaster* Aiton using metabolomics: Is it possible to identify the

- 1  
2  
3 748 region of origin of a pine from its metabolites? *Mol. Ecol.* 25, 959-976. doi:  
4 749 10.1111/mec.13525
- 5 750 Meijón, M., Rodríguez, R., Cañal, M.J., and Feito, I. (2009). Improvement of compactness and  
6 751 floral quality in azalea by means of application of plant growth regulators. *Sci. Hortic-  
7 752 Amsterdam* 119, 169-176. doi: 10.1016/j.scienta.2008.07.023
- 8 753 Miller, G., Shulaev, V., and Mittler, R. (2008). Reactive oxygen signaling and abiotic stress.  
9 754 *Physiol. Plantarum* 133, 481-489. doi: 10.1111/j.1399-3054.2008.01090.x
- 10 755 Mochida, K., and Shinozaki, K. (2011). Advances in omics and bioinformatics tools for systems  
11 756 analyses of plant functions. *Plant Cell Physiol.* 52, 2017-2038. doi: 10.1093/pcp/pcr153
- 12 757 Moon, J., Parry, G., and Estelle, M. (2004). The ubiquitin-proteasome pathway and plant  
13 758 development. *Plant Cell* 16, 3181-3195. doi: 10.1105/tpc.104.161220
- 14 759 Morel, A., Trontin, J.-F., Corbineau, F., Lomenech, A.-M., Beaufour, M., Reymond, I., et al. (2014).  
15 760 Cotyledonary somatic embryos of *Pinus pinaster* Ait. most closely resemble fresh,  
16 761 maturing cotyledonary zygotic embryos: biological, carbohydrate and proteomic  
17 762 analyses. *Planta* 240, 1075-1095. doi: 10.1007/s00425-014-2125-z
- 18 763 Morisseau, C. (2013). Role of epoxide hydrolases in lipid metabolism. *Biochimie* 95, 91-95. doi:  
19 764 10.1016/j.biochi.2012.06.011
- 20 765 Nguyen, A., Dormling, I., and Kremer, A. (1995). Characterization of *Pinus pinaster* seedling  
21 766 growth in different photo-and thermoperiods in a phytotron as a basis for early selection.  
22 767 *Scand. J. Forest Res.* 10, 129-139. doi: 10.1080/02827589509382876
- 23 768 Nguyen, T.Q., and Emery, R.N. (2017). Is ABA the earliest upstream inhibitor of apical  
24 769 dominance? *J. Exp. Bot.* 68, 881-884. doi: 10.1093/jxb/erx028
- 25 770 Paiva, J.A., Garcés, M., Alves, A., Garnier-Géré, P., Rodrigues, J.C., Lalanne, C., et al. (2008).  
26 771 Molecular and phenotypic profiling from the base to the crown in maritime pine  
27 772 wood-forming tissue. *New Phytol.* 178, 283-301. doi: 10.1111/j.1469-8137.2008.02379.x
- 28 773 Pascual, J., Cañal, M.J., Escandón, M., Meijón, M., Weckwerth, W., and Valledor, L. (2017).  
29 774 Integrated physiological, proteomic, and metabolomic analysis of ultra violet (UV) stress  
30 775 responses and adaptation mechanisms in *Pinus radiata*. *Mol. Cell. Proteomics* 16, 485-  
31 776 501. doi: 10.1074/mcp.M116.059436
- 32 777 Penterman, J., Zilberman, D., Huh, J.H., Ballinger, T., Henikoff, S., and Fischer, R.L. (2007). DNA  
33 778 demethylation in the Arabidopsis genome. *Proc. Natl. Acad. Sci. U.S.A* 104, 6752-6757.  
34 779 doi: 10.1073/pnas.0701861104
- 35 780 Pluskal, T., Castillo, S., Villar-Briones, A., and Orešič, M. (2010). MZmine 2: modular framework  
36 781 for processing, visualizing, and analyzing mass spectrometry-based molecular profile  
37 782 data. *BMC Bioinformatics* 11, 395. doi: 10.1186/1471-2105-11-395
- 38 783 Ponting, C.P., and Aravind, L. (1999). START: a lipid-binding domain in StAR, HD-ZIP and  
39 784 signalling proteins. *Trends Biochem. Sci.* 24, 130-132. doi: 10.1016/s0968-  
40 785 0004(99)01362-6
- 41 786 Proost, S., Van Bel, M., Vanechoutte, D., Van de Peer, Y., Inzé, D., Mueller-Roeber, B., et al.  
42 787 (2014). PLAZA 3.0: an access point for plant comparative genomics. *Nucleic Acids Res.*  
43 788 43, 974-981. doi: 10.1093/nar/gku986
- 44 789 R Development Core Team. (2015). *A Language and Environment for Statistical Computing:  
45 790 Vienna: R Foundation for Statistical Computing.*
- 46 791 Richards, D.E., King, K.E., Ait-Ali, T., and Harberd, N.P. (2001). How gibberellin regulates plant  
47 792 growth and development: a molecular genetic analysis of gibberellin signaling. *Ann.  
48 793 Rev. Plant Biol.* 52, 67-88. doi: 10.1146/annurev.arplant.52.1.67
- 49 794 Rivero, R.M., Ruiz, J.M., Garcia, P.C., Lopez-Lefebvre, L.R., Sánchez, E., and Romero, L. (2001).  
50 795 Resistance to cold and heat stress: accumulation of phenolic compounds in tomato and  
51 796 watermelon plants. *Plant Sci.* 160, 315-321. doi: 10.1016/S0168-9452(00)00395-2
- 52 797 Rocha, P.S., Sheikh, M., Melchiorre, R., Fagard, M., Boutet, S., Loach, R., et al. (2005). The  
53 798 Arabidopsis *HOMOLOGY-DEPENDENT GENE SILENCING1* gene codes for an S-  
54 799 adenosyl-L-homocysteine hydrolase required for DNA methylation-dependent gene  
55 800 silencing. *Plant Cell* 17, 404-417. doi: 10.1105/tpc.104.028332
- 56 801 Rohart, F., Gautier, B., Singh, A., and Lê Cao, K.-A. (2017). mixOmics: An R package for 'omics  
57 802 feature selection and multiple data integration. *PLoS Comput. Biol.* 13, e1005752. doi:  
58 803 10.1371/journal.pcbi.1005752
- 59 804 Romero-Rodríguez, M.C., Pascual, J., Valledor, L., and Jorrín-Novo, J. (2014). Improving the  
60 805 quality of protein identification in non-model species. Characterization of *Quercus ilex*  
61 806 seed and *Pinus radiata* needle proteomes by using SEQUEST and custom databases. *J.  
62 807 Proteomics* 105, 85-91. doi: 10.1016/j.jprot.2014.01.027

1  
2  
3  
4  
5  
6  
7  
8  
9  
10  
11  
12  
13  
14  
15  
16  
17  
18  
19  
20  
21  
22  
23  
24  
25  
26  
27  
28  
29  
30  
31  
32  
33  
34  
35  
36  
37  
38  
39  
40  
41  
42  
43  
44  
45  
46  
47  
48  
49  
50  
51  
52  
53  
54  
55  
56  
57  
58  
59  
60

- RStudio Team. (2016). *RStudio: Integrated development environment for R*. Boston, MA.
- Rüffer, M., Nagakura, N., and Zenk, M.H. (1978). Strictosidine, the common precursor for monoterpenoid indole alkaloids with 3  $\alpha$  and 3  $\beta$  configuration. *Tetrahedron Lett.* 18, 1593-1596. doi: 10.1016/S0040-4039(01)94613-1
- Sabatier, S., Baradat, P., and Barthelemy, D. (2003). Intra-and interspecific variations of polycyclism in young trees of *Cedrus atlantica* (Endl.) Manetti ex. Carrière and *Cedrus libani* A. Rich (Pinaceae). *Ann. For. Sci.* 60, 19-29. doi: 10.1051/forest:2002070
- Sadka, A., Dahan, E., Cohen, L., and Marsh, K.B. (2000). Aconitase activity and expression during the development of lemon fruit. *Physiol. Plantarum* 108, 255-262. doi: 10.1034/j.1399-3054.2000.108003255.x
- Sangster, T.A., and Queitsch, C. (2005). The HSP90 chaperone complex, an emerging force in plant development and phenotypic plasticity. *Curr. Opin. Plant Biol.* 8, 86-92. doi: 10.1016/j.pbi.2004.11.012
- Schmitz, A.J., Glynn, J.M., Olson, B.J., Stokes, K.D., and Osteryoung, K.W. (2009). *Arabidopsis* FtsZ2-1 and FtsZ2-2 are functionally redundant, but FtsZ-based plastid division is not essential for chloroplast partitioning or plant growth and development. *Mol. Plant* 2, 1211-1222. doi: 10.1093/mp/ssp077
- Schrack, K., Bruno, M., Khosla, A., Cox, P.N., Marlatt, S.A., Roque, R.A., et al. (2014). Shared functions of plant and mammalian StAR-related lipid transfer (START) domains in modulating transcription factor activity. *BMC Biology* 12, 70. doi: 10.1186/s12915-014-0070-8
- Sen, C.K., and Packer, L. (1996). Antioxidant and redox regulation of gene transcription. *Faseb J.* 10, 709-720. doi: 10.1096/fasebj.10.7.8635688
- Shannon, P., Markiel, A., Ozier, O., Baliga, N.S., Wang, J.T., Ramage, D., et al. (2003). Cytoscape: a software environment for integrated models of biomolecular interaction networks. *Genome Res.* 13, 2498-2504. doi: 10.1101/gr.1239303
- Singh, A., Gautier, B., Shannon, C.P., Rohart, F., Vacher, M., Tebutt, S.J., et al. (2018). DIABLO: from multi-omics assays to biomarker discovery, an integrative approach. *bioRxiv*. doi: 10.1101/067611
- Tanaka, H., Masuta, C., Uehara, K., Kataoka, J., Koiwai, A., and Noma, M. (1997). Morphological changes and hypomethylation of DNA in transgenic tobacco expressing antisense RNA of the S-adenosyl-L-homocysteine hydrolase gene. *Plant Mol. Biol.* 35, 981-986. doi: 10.1023/A:1005896711321
- Tariq, M., and Paszkowski, J. (2004). DNA and histone methylation in plants. *Trends Genet.* 20, 244-251. doi: 10.1016/j.tig.2004.04.005
- Thimm, O., Bläsing, O., Gibon, Y., Nagel, A., Meyer, S., Krüger, P., et al. (2004). MAPMAN: a user-driven tool to display genomics data sets onto diagrams of metabolic pathways and other biological processes. *Plant J.* 37, 914-939. doi: 10.1111/j.1365-313x.2004.02016.x
- Treutter, D. (2005). Significance of Flavonoids in Plant Resistance and Enhancement of Their Biosynthesis. *Plant Biol.* 7, 581-591. doi:10.1055/s-2005-873009
- Trontin, J.-F., Klimaszewska, K., Morel, A., Hargreaves, C., and Lelu-Walter, M.-A. (2016). "Molecular aspects of conifer zygotic and somatic embryo development: a review of genome-wide approaches and recent insights," in *In vitro embryogenesis in higher plants*. (Cham: Springer International Publishing AG), 167-207.
- Uggla, C., Magel, E., Moritz, T., and Sundberg, B. (2001). Function and dynamics of auxin and carbohydrates during earlywood/latewood transition in Scots pine. *Plant Physiol.* 125, 2029-2039. doi: 10.1104/pp.125.4.2029
- Valdés, A.E., Fernández, B., and Centeno, M.L. (2004). Hormonal changes throughout maturation and ageing in *Pinus pinea*. *Plant Physiol. Bioch.* 42, 335-340. doi: 10.1016/j.plaphy.2004.02.004
- Valledor, L., Carbó, M., Lamelas, L., Escandón, M., Colina, F.J., Cañal, M.J., et al. (2018). "When the tree let us see the forest: systems biology and natural variation studies in forest species" in *Progress in Botany*, eds Cánovas F., Lüttge U., Leuschner C., and Risueño MC (Cham: Springer International Publishing AG), 353-375.
- Valledor, L., Escandón, M., Meijón, M., Nukarinen, E., Cañal, M.J., and Weckwerth, W. (2014a). A universal protocol for the combined isolation of metabolites, DNA, long RNAs, small RNAs, and proteins from plants and microorganisms. *Plant J.* 79, 173-180. doi: 10.1111/tbj.12546

- 1  
2  
3 866 Valledor, L., and Jorrín, J. (2011). Back to the basics: maximizing the information obtained by  
4 867 quantitative two dimensional gel electrophoresis analyses by an appropriate experimental  
5 868 design and statistical analyses. *J. Proteomics* 74, 1-18. doi: 10.1016/j.jprot.2010.07.007  
6 869 Valledor, L., Jorrín, J.s.V., Rodríguez, J.L., Lenz, C., Meijón, M., Rodríguez, R., et al. (2010a).  
7 870 Combined proteomic and transcriptomic analysis identifies differentially expressed  
8 871 pathways associated to *Pinus radiata* needle maturation. *J. Proteome Res.* 9, 3954-3979.  
9 872 doi: 10.1021/pr1001669  
10 873 Valledor, L., Meijón, M., Hasbún, R., Cañal, M.J., and Rodríguez, R. (2010b). Variations in DNA  
11 874 methylation, acetylated histone H4, and methylated histone H3 during *Pinus radiata*  
12 875 needle maturation in relation to the loss of in vitro organogenic capability. *J. Plant Physiol.*  
13 876 167, 351-357. doi: 10.1016/j.jplph.2009.09.018  
14 877 Valledor, L., Pascual, J., Meijón, M., Escandón, M., and Cañal, M.J. (2015). Conserved epigenetic  
15 878 mechanisms could play a key role in regulation of photosynthesis and development-  
16 879 related genes during needle development of *Pinus radiata*. *PLoS One* 10, e0126405. doi:  
17 880 10.1371/journal.pone.0126405  
18 881 Valledor, L., Romero-Rodríguez, M.C., and Jorrin-Novo, J.V. (2014b). "Standardization of data  
19 882 processing and statistical analysis in comparative plant proteomics experiment," in *Plant*  
20 883 *Proteomics*. (Cham: International Publishing Springer AG), 51-60.  
21 884 Valledor, L., and Weckwerth, W. (2014). "An improved detergent-compatible gel-fractionation LC-  
22 885 LTQ-Orbitrap-MS workflow for plant and microbial proteomics," in *Plant Proteomics:*  
23 886 *Methods and Protocols*. (Cham: Springer International Publishing AG), 347-358.  
24 887 Vázquez-González, C., López-Goldar, X., Zas, R., and Sampedro, L. (2019). Neutral and climate-  
25 888 driven adaptive processes contribute to explain population variation in resin duct traits in  
26 889 a mediterranean pine species. *Front. Plant Sci.* 10, 1-12. doi: 10.3389/fpls.2019.01613  
27 890 Verdú, M., and Climent, J. (2007). Evolutionary correlations of polycyclic shoot growth in *Acer*  
28 891 (*Sapindaceae*). *Am. J. Bot.* 94, 1316-1320. doi: 10.3732/ajb.94.8.1316  
29 892 Vimont, N., Schwarzenberg, A., Domijan, M., Beauvieux, R., Arkoun, M., Jamois, F., et al. (2019).  
30 893 Hormonal balance finely tunes dormancy status in sweet cherry flower buds. *bioRxiv*,  
31 894 423871. doi: 10.1101/423871  
32 895 Vizcaíno-Palomar, N., Ibáñez, I., González-Martínez, S.C., Zavala, M.A., and Alía, R. (2016).  
33 896 Adaptation and plasticity in aboveground allometry variation of four pine species along  
34 897 environmental gradients. *Ecol. Evol.* 6, 7561-7573. doi: 10.1002/ece3.2153  
35 898 Wang, W., Vinocur, B., Shoseyov, O., and Altman, A. (2004). Role of plant heat-shock proteins  
36 899 and molecular chaperones in the abiotic stress response. *Trends Plant Sci.* 9, 244-252.  
37 900 doi: 10.1016/j.tplants.2004.03.006  
38 901 Woo, E.-J., Dunwell, J.M., Goodenough, P.W., Marvier, A.C., and Pickersgill, R.W. (2000).  
39 902 Germin is a manganese containing homo-hexamer with oxalate oxidase and superoxide  
40 903 dismutase activities. *Nat. Struct. Mol. Biol.* 7, 1036. doi: 10.1038/80954  
41 904 Zas, R., and Fernández-López, J. (2005). Juvenile genetic parameters and genotypic stability of  
42 905 *Pinus pinaster* Ait. open-pollinated families under different water and nutrient regimes.  
43 906 *For. Sci.* 51, 165-174. doi: 10.1093/forestscience/51.2.165  
44 907 Zas, R., Merlo, E., and Fernández-López, J. (2004). Genetic parameter estimates for Maritime  
45 908 pine in the Atlantic coast of North-west Spain. *For. Genet.* 11, 45-53. doi: 10.261/101373  
46 909 Zhang, C.-J., Zhao, B.-C., Ge, W.-N., Zhang, Y.-F., Song, Y., Sun, D.-Y., et al. (2011). An  
47 910 apoplastic h-type thioredoxin is involved in the stress response through regulation of the  
48 911 apoplastic reactive oxygen species in rice. *Plant Physiol.* 157, 1884-1899. doi:  
49 912 10.1104/pp.111.182808  
50 913 Zheng, C., Halaly, T., Acheampong, A.K., Takebayashi, Y., Jikumaru, Y., Kamiya, Y., et al. (2015).  
51 914 Abscisic acid (ABA) regulates grape bud dormancy, and dormancy release stimuli may  
52 915 act through modification of ABA metabolism. *J. Exp. Bot.* 66, 1527-1542. doi:  
53 916 10.1093/jxb/eru519  
54 917 Zhu, H., Qian, W., Lu, X., Li, D., Liu, X., Liu, K., et al. (2005). Expression patterns of purple acid  
55 918 phosphatase genes in *Arabidopsis* organs and functional analysis of *AtPAP23*  
56 919 predominantly transcribed in flower. *Plant Mol. Biol.* 59, 581-594. doi: 10.1007/s11103-  
57 920 005-0183-0  
58 921 Zimmerman, J.L. (1993). Somatic embryogenesis: a model for early development in higher plants.  
59 922 *Plant Cell* 5, 1411. doi: 10.1105/tpc.5.10.1411  
60 923  
61 924

## 925 **FIGURE LEGENDS**

926 **Figure 1.** Plant material employed in this analysis. Two-year old seedlings exhibiting an apical  
927 bud with young (**A**) or mature (**B**) morphology. Comparison of young (left) and mature (right) buds  
928 (**C**). Dissection of young (left) and mature (right) buds into their apical and basal parts (**D**). Vertical  
929 bars represent 0.5 cm length.

930  
931 **Figure 2.** Venn diagrams showing the qualitative differences between bud sections and ontogenic  
932 stages at proteome (**A**) and metabolome (**B**) levels. Heatmap clustering of proteins (**C**) and  
933 metabolites (**D**) classified according to Mapman categories. Distances were established  
934 employing Manhattan distance and aggregated according to Ward's method.

935  
936 **Figure 3.** Integrative analysis of proteome and metabolome. (**A**) Plot of samples scores at  
937 proteome and metabolome levels, showing components 1 and 2 in horizontal and vertical axes,  
938 respectively, (**B**) integrative heatmap clustering, (**C**) loadings plot showing the proteins with  
939 greatest correlation to components 1 and 2, (**D**) and loadings plot showing the metabolites with  
940 greatest correlation to components 1 and 2. Color code of the horizontal bar of the heatmap  
941 represents proteins (cyan) or metabolites (purple), while vertical shows treatments. Euclidean  
942 distances and complete-linkage algorithms were employed for classifying samples. Color of the  
943 protein loading bars represent the treatment with higher protein abundance.

944 **Figure 4.** Integrative analysis of proteome and metabolome during bud maturation. (**A**) sPLS-  
945 based network built after DIABLO analysis. Correlation cut-off was 0.75 and edge color reflect  
946 positive (red) or negative (green) interactions. Node color indicate Mapman functional bin and  
947 shape indicate proteins (circle) or metabolites (square). Same representations in which node color  
948 indicates that protein/metabolite is more abundant in (**B**) one of the treatments, (**C**) in the  
949 apical/basal part of the bud, or (**D**) in mature/young buds.

950 **Figure 5.** Whisker box representation of the qPCR analysis of target genes in the different bud  
951 sections. Dots indicate expression values of the different biological replicates normalized vs the  
952 expression of control genes ( $\Delta\text{Cq Target}/\Delta\text{Cq Controls}$ ). Significant differences between bud  
953 sections and developmental status (ANOVA/Tukey HSD,  $p < 0.001$ ) were highlighted (\*\*\*)  
954



1 **Title:** Proteometabolomic characterization of apical bud maturation in

2 *Pinus pinaster*

3  
4 **Running Title:** Proteometabolomic characterization of apical bud

5  
6  
7 Luis Valledor\*, Sara Guerrero, Lara García-Campa, Mónica Meijón\*

8  
9 Plant Physiology, Department of Organisms and Systems Biology, University of

10 Oviedo, Oviedo 33071, Asturias, Spain

11 \*Corresponding authors: [valledorluis@uniovi.es](mailto:valledorluis@uniovi.es); [meijonmonica@uniovi.es](mailto:meijonmonica@uniovi.es)

12  
13  
14  
15 **KEYWORDS:** Conifer, Bud aging, Metabolomics, Proteomics, Integrative approach

16  
17 **Number of words:** 106~~4753~~

18 **Number of words:** 65~~5560~~ (without References, Funding, Acknowledgments)

19 **Number of figures included in manuscript:** 5

20 **Number of Supplementary figures:** 1 (S1)

21 **Number of Supplementary tables:** 5 (S1 to S5)

22

23 **ABSTRACT (300 words)**

24 Bud maturation is a physiological process which implies a set of morphophysiological changes  
25 which lead to the transition of growth patterns from [juvenileyoung](#) to [adultmature](#). This transition  
26 defines tree growth and architecture, and in consequence traits such as biomass production and  
27 wood quality. In *Pinus pinaster*, a conifer of great timber value, bud maturation is closely related  
28 to polycyclism (multiple growth periods per year). This process causes a lack of apical dominance,  
29 and consequently increased branching that reduces its timber quality and value. However, despite  
30 its importance, little is known about bud maturation. In this work, proteomics and metabolomics  
31 were employed to study apical and basal sections of [juvenileyoung](#) and [adultmature](#) buds in *P.*  
32 *pinaster*. Proteins and metabolites in samples were described and quantified using (n)UPLC-LTQ-  
33 Orbitrap. The datasets were analyzed employing an integrative statistical approach, which  
34 allowed the determination of the interactions between proteins and metabolites and the different  
35 bud sections and ages. Specific dynamics of proteins and metabolites such as HISTONE H3 and  
36 H4, RIBOSOMAL PROTEINS L15 and L12, CHAPERONIN TCP1, 14-3-3 protein gamma,  
37 gibberellins A1, A3, A8, strigolactones and ABA, involved in epigenetic regulation, proteome  
38 remodeling, hormonal signaling and abiotic stress pathways showed their potential role during  
39 bud maturation. Candidates and pathways were validated employing interaction databases and  
40 targeted transcriptomics. These results increase our understanding of the molecular processes  
41 behind bud maturation a key step towards improving timber production and natural pine forests  
42 management in a future scenario of climate change. However, [further](#) studies are necessary by  
43 using different *P. pinaster* populations that show [contrastinant](#) wood quality and stress tolerance  
44 in order to generalize the results.

45

## 46 INTRODUCTION

47 Pines are key players of forest ecosystems since most ~~of the~~ species have the ability to colonize  
48 a great variety of niches, act as good CO<sub>2</sub> sinks due to its fast growth (Allona et al., 1998), and  
49 are demanded by forest industry due to their quality timber, paper pulp and resins (Canales et al.,  
50 2014). Current production is not enough to cover current and predicted timber demand (FAO,  
51 2009) and new strategies should be designed for implementing a more sustainable forest  
52 management also considering the climate change scenario (FAO, 2015). The use of fast-growth  
53 species such as *Pinus pinaster* Aiton, commonly known as maritime pine, may have an important  
54 role to this aim. This species has a major ecological and industrial role in southern Europe both  
55 at Mediterranean and Atlantic basins (González et al., 2016; Meijón et al., 2016; Cano et al.,  
56 2018). Its provenances adapted to different geoclimatic conditions across its distribution exhibit  
57 specific adaptations, allowing its optimal growth under a wide range of environments, from mild  
58 humid Atlantic regions to warm dry Mediterranean. These adaptations are genetically encoded,  
59 having this species a great genetic variability (Meijón et al., 2016; Vizcaíno-Palomar et al., 2016;  
60 Vázquez-González et al., 2019).

61 However, ~~the architecture of this species can be greatly affected by harsh environmental~~  
62 ~~conditions like drought periods, which can ultimately affect tree productivity despite its great~~  
63 ~~adaptive capacity, the productivity of this species is greatly affected by environmental conditions~~  
64 ~~and specifically drought periods since they can greatly alter tree architecture.~~ *Pinus pinaster* is a  
65 species with a characteristic polycyclic growth (multiple shoot flushes in a single season) (Zas et  
66 al., 2004). This growth pattern, which reduces tree value due to a loss of apical dominance and  
67 increased branching, is inheritable and genetically conditioned, with provenances more polycyclic  
68 than others (Sabatier et al., 2003; Zas et al., 2004; Meijón et al., 2016). Polycyclism also presents  
69 an important environmental component, being conditioned by water availability, soil composition  
70 or radiation (Sabatier et al., 2003; Girard et al., 2011). It has been shown that periods of drought  
71 reduce its appearance and also tree growth, and that fertile soils and good irradiation lead to  
72 increase growth cycles and branching (Sabatier et al., 2003; Verdú and Climent, 2007).  
73 Polycyclism is also conditioned by the maturation state of the apical bud (Sabatier et al., 2003;  
74 Girard et al., 2011), being buds with ~~juvenileyoung~~ phenology more polycyclic than ~~adultmature~~,  
75 although the molecular mechanisms that explain these differences have not yet been described.

76 Bud maturation implies a number of phenological changes, altering growth pattern,  
77 morphogenetic competence and increasing abiotic stress resistance (Jordy, 2004; Brunner et al.,  
78 2017). Maturation is regulated by internal and environmental factors. Among internal factors, plant  
79 hormones (Meijón et al., 2009) and epigenetic mechanisms regulating differential gene  
80 expression are required for bud maturation (Valledor et al., 2010b; Valledor et al., 2015; Conde  
81 et al., 2017). This differential gene expression should lead to changes in proteome and, in  
82 consequence, in metabolome, altogether resulting in the physiological and morphological  
83 characteristics of each ontogenetic age (Haffner et al., 1991; Meijón et al., 2016; Großkinsky et  
84 al., 2017). Surprisingly, and despite its importance for adaptive responses, tree growth or

1  
2  
3 85 polycyclism, little is known about the molecular processes that are behind bud maturation process  
4 86 and different developmental stages and how they interact with environment. The great complexity  
5 87 that these processes seem to have along with the large number of variables potentially involved  
6 88 and not previously described suggest an unmanaged and massive strategy as the most  
7 89 appropriate to address this problem.

10  
11 90 The availability of high throughput alternatives for molecular phenotyping such as gel-free  
12 91 proteomics and metabolomics give us an unprecedented capability to address this gap (Valledor  
13 92 et al., 2018). These techniques usually associated to model species can currently be applied with  
14 93 high confidence in almost any organism, since they do not require extended genome information.  
15 94 Despite unsequenced, *Pinus pinaster* has extensive transcriptomic data available that ease  
16 95 protein identification (Romero-Rodríguez et al., 2014). In this species, there are several  
17 96 contributions in the proteomics field but focused on the study of wood forming tissues (Paiva et  
18 97 al., 2008; Garcés et al., 2014) and somatic embryogenesis (Morel et al., 2014; Trontin et al.,  
19 98 2016). As the final reflection of genomes and its variation, metabolome analyses allowed to define  
20 99 population structures and evolution in this species (Meijón et al., 2016; López-Goldar et al., 2019),  
21 100 and also [adaptive responses to abiotic/biotic stress responses to abiotic/biotic stress and](#)  
22 101 [adaption](#) (Cañas et al., 2015; de Simón et al., 2017; López-Goldar et al., 2020). The combination  
23 102 of different omics greatly increases the power of analysis since the datasets of the different levels  
24 103 complement each other in a synergistic way (Mochida and Shinozaki, 2011; Kim et al., 2012).  
25 104 This type of integrative studies has already been carried out successfully in conifers to study  
26 105 needle development combining proteomics and transcriptomics (Valledor et al., 2010a) or to  
27 106 comprehensively analyze response to heat (Escandón et al., 2017) or ultraviolet stress comparing  
28 107 proteomics and metabolomics (Pascual et al., 2017). However, there is no information related to  
29 108 bud maturation in pines.

30  
31 109 Therefore, the main aim of this work was to study the bud maturation process in *Pinus pinaster*  
32 110 using integrative omics approach combining proteomics and metabolomics. The integration of  
33 111 both levels allowed the extensive characterization of bud maturation processes. Specific  
34 112 dynamics of proteins and metabolites related to epigenetic regulation, proteome remodeling,  
35 113 hormonal signaling, and abiotic stress response (such as histones, ribosomal proteins,  
36 114 strigolactones, gibberellins, ABA, and chaperones) showed an essential role during bud  
37 115 maturation. In addition, the interconnection of these elements and its relation to different polycyclic  
38 116 capacity and stress tolerance of each maturation state of the bud was revealed through an  
39 117 integrative approach.

## 118 MATERIAL AND METHODS

### 119 Plant material and growth conditions

120 Apical buds in young and mature stages were sampled from two-years-old *Pinus pinaster*  
121 seedlings (plant size [about around](#)  $20 \pm 3$  cm) just after they exhibited young/mature apical phase  
122 change. These plants were grown in a greenhouse with seasonal fertirrigation.

1  
2  
3 123 Buds in the young stage show leaf primordia differentiate into photosynthetically active primary  
4 124 needles around of [the shoot apical meristem \(SAM\)](#). However, when ~~it is reached~~ the mature  
5  
6 125 stage [is reached](#), leaf primordia differentiate into scale leaves, and photosynthetic activity is  
7  
8 126 shifted to long needles differentiated on brachyblasts in more distal positions on the stem (Jordy,  
9 127 2004). Apical buds of 18 seedlings of the same age, half of them having mature morphology and  
10 128 half of them young, were sampled and dissected into their apical and basal sections,  
11 129 corresponding to apical and axillary/foiar meristems, respectively (Figure 1). Three biological  
12 130 replicates for each treatment (apical and basal parts of the bud, young and mature buds) were  
13 131 constituted pooling basal or apical parts of the buds of three different seedlings with the same  
14 132 bud developmental stage. Samples were immediately frozen in liquid nitrogen and kept at -80 °  
15 133 C until biomolecule extraction. Metabolites, proteins, and RNA were isolated from the same  
16 134 sample following the protocol of Valledor et al. (2014a) using 75 mg of fresh weight per sample.

### 21 135 **Metabolome analysis**

22  
23 136 High-performance liquid chromatography (Dionex Ultimate 3000, ThermoFisher Scientific, USA)  
24 137 was coupled to a LTQ-Orbitrap XL high resolution mass spectrometer equipped with a HESI II  
25 138 (heated electrospray ionization) source and controlled by Xcalibur version 2.2 (Thermo Fisher  
26 139 Corporation). Polar fraction of each sample was analyzed twice, first using the positive and then  
27 140 the negative ion modes. Samples were run according to the procedure described by Meijón et al.  
28 141 (2016). Instrument was operated in full-scan mode with a resolution of 60 000, and spectra were  
29 142 acquired in mass range  $m/z$  50–1000 in the positive mode, and 65–1000 in the negative mode.  
30 143 The resolution and sensitivity were controlled by the injection of a standard mix (caffeine, proline,  
31 144 and sucrose) after the analysis of each batch and resolution was also checked with the aid of lock  
32 145 masses (phthalates). Blanks were also analyzed during the sequence. With the aim of improving  
33 146 metabolite assignment, one sample of each treatment was additionally reanalyzed including an  
34 147 ion fragmentation step. Chromatographic and analytical conditions were the same, but top-three  
35 148 ions of each scan were fragmented (30 s dynamic exclusion window). Parent ions (minimum  
36 149 intensity of 500) were fragmented by CID (normalized collision energy of 35, activation Q 0.25,  
37 150 and activation time 90 ms). These spectra were employed for MS/MS metabolite identification as  
38 151 described below.

39 152 RAW files were directly processed employing MZMINE v2.14 (Pluskal et al., 2010). Spectra were  
40 153 filtered establishing noise threshold at  $2 \times 10^4$  and minimum peak height at  $2.5 \times 10^5$ . Peaks were  
41 154 smoothed and deconvoluted using a local minimum search algorithm (95 % chromatographic  
42 155 threshold, minimum retention range 0.2 min, minimum relative height of 5 %, and minimum ratio  
43 156 top/edge of 0.5). Chromatograms were aligned using the RANSAC algorithm with a tolerance of  
44 157 5 ppm of  $m/z$  and 0.2 min of retention time. Peak areas were used for quantification.

45  
46  
47 158 Peaks were identified following a sequential approach. The first stage was performed against our  
48 159 in-house library (>100 compounds) and manual annotation considering its  $m/z$  and retention  
49 160 times. In a second stage, MS/MS data was used for identification employing Compound

1  
2  
3 161 Discoverer software (Thermo Scientific, USA) and custom scripts for comparing experimental  
4 162 data to MS/MS databases Metlin, HMDB and FooDB. A positive identification was defined when  
5 163 parent mass was below 5-ppm threshold compared to analyte in DB and at least, two main ions  
6 164 of fragmentation spectra were identified. The last stage assigned potential identity to masses by  
7 165 direct comparison of ion masses using a 5-ppm threshold and KEGG, HMDB, FooDB, Plantcyc,  
8 166 and MassBank databases. Those metabolites that were defined after the comparison with our  
9 167 standard compound library or by a matching of MS/ MS were considered as unquestionably  
10 168 'identified', while were considered 'tentatively assigned' those molecular ions with exact masses  
11 169 corresponding to identified metabolites in databases. Metabolite identification against our library  
12 170 was confirmed by RT, mass, and isotopic patterns.

### 171 **Protein identification and quantitation using nLC-Orbitrap-MS analysis**

172 Sixty µg of total protein were cleaned, digested, and desalted following the protocol described by  
173 Valledor and Weckwerth (2014). Peptide chromatography and mass spectrometric analysis were  
174 performed according to Pascual et al. (2017) with only a slight modification in the effective  
175 gradient, which was set to 90 min from 5 % to 45 % acetonitrile/0.1 % formic acid (v:v) with a later  
176 column regeneration step of 27 min. The employed column was a Chromolith RP-18R 15 cm  
177 length 0.1 cm inner diameter (Merck, Germany).

178 Spectra were processed in Proteome Discoverer 2.0 (Thermo Scientific, USA). Protein  
179 identification threshold was established at 5% and 1% false discovery rates (FDR) at peptide and  
180 protein levels, respectively. Only proteins with at least two identified peptides and one of them  
181 unique were considered as identified. Four databases were used: *Pinus sylvestris* and *Pinus*  
182 *taeda* (34063 accessions) (Proost et al., 2014), and against in-house databases, *Pinus pinaster*  
183 (117080 accessions) and *Pinus radiata* (67647 accessions) that were built following the  
184 procedure described by Romero-Rodríguez et al. (2014). Proteins were also functionally  
185 classified according to Mapman (Thimm et al., 2004) functional bins. Identified proteins were  
186 quantified by a label-free approach based on the estimation of the areas of the three most  
187 abundant peaks assigned to each protein by Proteome Discoverer.

### 188 **Targeted transcriptomic analysis of candidate genes**

189 RNA abundance was determined in a microdrop spectrophotometer NB1 (Nabi, South Korea) and  
190 its integrity was checked by agarose gel electrophoresis. One µg of RNA was reversed  
191 transcribed using the RevertAid kit (Thermo Scientific, USA) and random hexamers as primers  
192 following the manufacturer's instructions. qPCR reactions were performed in a CFX96™ Real-  
193 Time System (Biorad, USA) with RealQ Plus Master Mix Green, no ROX (2X) (Ampliqon,  
194 Denmark); four biological and two analytical replicates per treatment were made for each gene.  
195 Expression levels of *GLYCERALDEHYDE 3-PHOSPHATE DEHYDROGENASE (GAPDH)* and  
196 *UBIQUITINE (UBI)* were used as endogenous control and the results were analyzed by Bio-Rad  
197 CFX Manager 3.1 (Biorad, USA) software using the cycle threshold comparative method ( $\Delta C_T$ ).

1  
2  
3 198 Detailed information about the primers used for qPCR experiments is available in Supplementary  
4 199 Table S1.

## 200 **Statistical and bioinformatics analysis**

201 All statistical procedures were conducted with the R programming language running under the  
202 open source computer software R v3.5.0 (R Development Core Team, 2015) and RStudio  
203 v1.1.423 (RStudio Team, 2016) using the packages pRocesomics<sup>1</sup> and mixOmics (Rohart et al.,  
204 2017).

205 Three biological replicates per treatment were used for metabolome and proteome analysis.  
206 Proteome and metabolome datasets were pre-processed following the recommendations of  
207 Valledor and Jorrín (2011) and Valledor et al. (2014b). In brief, missing values were imputed using  
208 a Random Forest approach, and variables were filtered out if they were not present in at least all  
209 of replicates corresponding to one treatment or in at least 45% of the analyzed samples. Data  
210 were normalized and transformed following a samplecentric approach followed by log  
211 transformation. Centered and scaled values (z-scores) were subjected to univariate (one-way  
212 ANOVA followed by a Tukey HSD post-hoc test, P<0.05.) and Venn diagrams, and heat map  
213 clustering. To avoid variable noise only those variables with interquartile range 50% greater than  
214 average were selected for multivariate analyses. Integrative analysis was based on the use of  
215 DIABLO algorithm and network representation. Cytoscape v. 3.7 (Shannon et al., 2003) was  
216 employed in network representation and analysis. Proteins were annotated according to Mapman  
217 classification employing protein sequences and Mercator online tool v3.6 (Lohse et al., 2014)  
218 while metabolites were manually classified according to this classification.

## 219 **RESULTS**

### 220 **Proteomic and metabolomic characterization of buds in *Pinus pinaster***

221 Proteomic analyses of [juvenile/young](#) and [adult/mature](#) buds and their sections allowed the  
222 identification of 1609 proteins. Proteins were annotated according to Mapman, classifying 1540  
223 proteins in 34 functional bins. 951 proteins showed abundances and consistencies above  
224 threshold for their use in quantitative analyses. Out of these, 142 were differentially accumulated  
225 between treatments (ANOVA p-value <0.05; Supplementary Table S2). At metabolome level,  
226 3670 peaks were detected, being 2267 suitable for quantification (Supplementary Table S3).  
227 From these, 133 peaks were unequivocally identified using the in-house database or MS/MS  
228 spectra, corresponding to 105 unique compounds, and 974 were tentatively assigned by  
229 comparing their very accurate masses to those available in public databases (Supplementary  
230 Table S4). 75 metabolites were classified according to Mapman. Despite the high number of  
231 identified/assigned metabolites, their complete classification according to Mapman was not  
232 possible, mainly due to the difficulty of classifying secondary metabolites. However, this potential  
233 bias does not affect the most studied and preserved functional groups such as those related to

---

<sup>1</sup> <https://github.com/Valledor/pRocesomics>

234 primary metabolism. From all detected compounds, 914 were differentially expressed between  
235 analyzed samples (ANOVA 5% FDR; Supplementary Table S3).

236 Venn analyses revealed qualitative differences between ontogenic stages and bud sections. At  
237 protein level (Figure 2A), [juvenileyoung](#) buds (apical and basal sections) showed the highest  
238 number of characteristic proteins (126) but, interestingly, the apical section of the [adultmature](#)  
239 bud was the most differentiated organ with 59 characteristic proteins. At metabolome level (Figure  
240 2B), [adultmature](#) tissues showed the highest rate of unique compounds (569), while the apical  
241 section of the [juvenileyoung](#) bud exhibited the highest number of characteristic metabolites (194).

242 Quantitative analyses of Mapman classified proteins (Figure 2C) and metabolites (Figure 2D)  
243 pointed the differential pathways among bud sections and developmental stages. At proteome  
244 level, increased pathway clusters related to stress, hormone, lipidic, energetic, and major  
245 carbohydrate metabolism pathways can be correlated to the different tissues that were analyzed.  
246 Heatmap classified samples according to bud section, which may be suggesting a greater  
247 variation between apical and basal meristem proteomes than between [adultmature](#) and  
248 [juvenileyoung](#) bud proteomes. Contrary to proteome, metabolome allowed the classification of  
249 samples in relation to their ontogenetic age. This metabolomic differentiation was mainly caused  
250 by differences in photosynthesis, aminoacid synthesis and metabolism, redox regulation, and  
251 nucleotide metabolism.

252 These differences between [adultmature](#) and [juvenileyoung](#) buds and their basal and apical  
253 sections may be related to the location of the shoot apical meristem (SAM) activity in the apical  
254 section of the bud and also to the differential growth and developmental patterns of [juvenileyoung](#)  
255 and [adultmature](#) buds, as it was demonstrated by the differential accumulation of sample-specific  
256 pathways. Furthermore, the accumulation of a higher number of specific metabolites in  
257 comparison to proteins revealed the potential effect over the metabolome of the changes related  
258 to a smaller number of proteins. Alterations of key enzymes of metabolic pathways may lead to  
259 changes in abundance of a large number of metabolites. On the other hand, samples with a great  
260 ontogenic and functional differentiation ([juvenileyoung](#) vs [adultmature](#)) shared numerous  
261 proteins, which diffculted their classification according to their developmental stage. However,  
262 metabolites allowed their classification, reflecting the importance of metabolomic specificity in  
263 functional differentiation. The metabolome is the final downstream product of gene transcription  
264 and, therefore, changes in it are amplified relative to the changes in transcriptome and proteome  
265 (Das et al., 2015; Escandón et al., 2017). As [juvenileyoung](#) buds present more active  
266 development than differentiated [adultmature](#) buds, it is expected an overaccumulation of  
267 metabolites related to active processes of development, such as redox activity or aminoacid  
268 synthesis.

269

270 **The integrative analysis of proteome and metabolome unmasked potential**  
271 **interaction networks involved in bud maturation and differentiation in *Pinus***  
272 ***pinaster***



1  
2  
3 273 The combination of different omic levels in an integrative analysis supposes a major analytical  
4 274 advantage since the different levels can be used for cross-validation and, at the same time, to get  
5 275 a global overview of the physiological processes (Singh et al., 2018). For this purpose, we  
6 276 employed DIABLO algorithm (Rohart et al., 2017) to analyze proteome and metabolome datasets  
7 277 (Figure 3). This approach provided a better clustering of the samples at proteome and  
8 278 metabolome levels (Figure 3A). The joint analysis of both datasets correctly classified studied  
9 279 tissues (Figure 3B). The basis of this classification relied on the biological source of variation  
10 280 gathered by two main components, which collectively accounted 59% of the total variance  
11 281 (Supplementary Table S5). The analysis of the variables exhibiting highest loadings to these  
12 282 components (Figure 3C-D; Supplementary Table S5) allowed a biological interpretation of these  
13 283 results.

14 284 Component 1 gathered the variation related to ontogenic differentiation, distinguishing between  
15 285 [juvenileyoung](#) and mature buds. Enzymes related to energy, protein biosynthesis, lipid  
16 286 metabolism, and signaling/differentiation showed the highest correlations to this component  
17 287 (Figure 3C). [JuvenileYoung](#) tissues were characterized by an increased accumulation of energy-  
18 288 related ATPases or PSII reaction center proteins as well as several ribosomal- and RNA-related  
19 289 proteins. Lipids are supposed to be relevant players in this differentiation, and despite no  
20 290 differential lipids were identified after metabolome analysis, enzymes related to their metabolism  
21 291 were key nodes of our models. ACETYLCOA CARBOXYLASE CARBOXYL TRANSFERASE  
22 292 SUBUNIT ALPHA, which is a key lipidic enzyme as seen above (Harwood, 1996), a START-like  
23 293 domain, whose function in lipid regulation in plants was previously suggested (Ponting and  
24 294 Aravind, 1999), and GDSL ESTERASE LIPASE, being described its function in development,  
25 295 defense, synthesis of secondary metabolites, and morphogenesis in some plant species  
26 296 (Chepyshko et al., 2012), were some of the most highlighted lipidic-related enzymes.

27 297 On the other hand, RAS proteins, 14-3-3 transcription factors and DNA regulatory proteins by  
28 298 epigenetic mechanisms were re-emphasized as key processes in bud differentiation (Figure 3B).  
29 299 HISTONE 3 and HISTONE 4 (Tariq and Paszkowski, 2004; Valledor et al., 2010b; Bräutigam et  
30 300 al., 2013), GLYCOSYL HYDROLASES FAMILY 100 (Penterman et al., 2007), and RAS related  
31 301 proteins (Kamada et al., 1992; Alonso et al., 2007) regulate developmental processes, and were  
32 302 important to explain the ontogenic differences in the analyzed tissues. Many of these proteins  
33 303 were correlated to primary and secondary metabolites, some of which are characteristic of specific  
34 304 physiological stages, and therefore, having a potential involvement in development. Even though  
35 305 none of the most significant metabolites were identified in public databases, it would be interesting  
36 306 to highlight some of them due to their possible importance in differentiation interaction networks.  
37 307 Specifically, in ontogenic differentiation, significant metabolites (P0340, N1518, P0320, and  
38 308 N1292) seemed to differentiate [juvenileyoung](#) from [adultmature](#) buds (Figure 3D; Supplementary  
39 309 Table S5).

40 310 Second component distinguished between the apical and basal parts of the bud. Enzymes related  
41 311 to protein biosynthesis and folding-related, as well as peroxidases, were characteristic of this

1  
2  
3 312 component (Figure 3C). Apical sections of the bud showed a positive correlation, and were  
4 313 characterized by increased abundance of stress-related proteins such as CHAPERONIN-LIKE  
5 314 TCP1 and others (Wang et al., 2004), a MANGANESE BINDING SITE from a GERMIN, which is  
6 315 related to abiotic and biotic stresses response in plants (Woo et al., 2000), and a PEROXIDASE.  
7  
8 316 On the other hand, key variables defining the basal parts of the buds showed negative correlation  
9 317 to this component. Basal sections were characterized by higher growth and proliferation rates  
10 318 than apical, fact that explains the importance of proteins related to cell division and reorganization  
11 319 such as PROFILIN 1 or PROHIBITIN 1 in this model. This last protein was only found in basal  
12 320 sections of [adultmature](#) bud, having multiple functions related to plant development and stress  
13 321 tolerance (Chen et al., 2005). In the same way, several transferases such as PYRIDOXAL  
14 322 PHOSPHATE DEPENDENT TRANSFERASE or PHOSPHORIBOSYLGLYCINAMIDE  
15 323 FORMYLTRANSFERASE were characteristic of the basal section of the bud. Most of the  
16 324 metabolites associated to this component were not identified. Among identified metabolites,  
17 325 loganin and deoxyloganin were only detected in apical sections of the bud, while basal had only  
18 326 highlighted unidentified metabolites (P1560 + P1340, N2243 and P1379) (Figure 3D;  
19 327 Supplementary Table S5).

20  
21  
22  
23  
24  
25  
26 328 The clustering and heatmap visualization of this integrative analysis (Figure 3B; Supplementary  
27 329 Figure S1) complemented results described above, revealing four different sets of variables:  
28 330 those proteins and metabolites over-accumulated in apical section of [juvenileyoung](#) bud and  
29 331 down-accumulated in the rest of the samples; those over-accumulated in basal section of  
30 332 [juvenileyoung](#) bud and down-accumulated in the rest of the samples; those over-accumulated in  
31 333 [juvenileyoung](#) buds and not in [adultmatures](#); and those over-accumulated in [adultmature](#) buds but  
32 334 not in [juvenileyoung](#) ones. First set of variables was mainly composed by metabolites and proteins  
33 335 already referenced such as GERMIN MANGANESE BINDING PROTEIN,  
34 336 PHOSPHOGLUCONATE DEHYDROGENASE or ribosomal proteins; conversely, second set of  
35 337 proteins was essentially constituted by proteins from different metabolic pathways such as  
36 338 photosynthesis, redox mechanism or signaling. Above all the differential variables found in the  
37 339 third set of proteins, this group was characterized by numerous proteins belonging on the one  
38 340 hand to stress pathways such as the previously described CPN10 or H-TYPE THIOREDOXIN  
39 341 (Zhang et al., 2011) and EPOXIDE HYDROLASE (Morisseau, 2013) like proteins, and on the  
40 342 other hand, to energetic routes with a large number of proteins identified (ATP-DEPENDENT 6-  
41 343 PHOSPHOFRUCTOKINASE 2, MALATE DEHYDROGENASE, CYTOCHROME C, V-TYPE  
42 344 PROTON ATPase SUBUNIT D, SUCCINATE DEHYDROGENASE UBIQUINONE  
43 345 FLAVOPROTEIN SUBUNIT). Likewise, previously highlighted proteins related to lipid metabolism  
44 346 (ACETYL-COA ACETYLTRANSFERASE) and cellular reorganization (PROFILIN 1 and  
45 347 PROHIBITIN 1) were found in this pattern. Last set, including those proteins characteristic of  
46 348 [adultmature](#) buds, differentiation was established by a large number of non-identified metabolites  
47 349 and a small number of proteins, including ribosomal proteins, 14-3-3, HISTONE H3 or  
48 350 GLYCOSYL HYDROLASE FAMILY 100 previously described.  
49  
50  
51  
52  
53  
54  
55  
56  
57  
58  
59  
60

1  
2  
3 352 **The analysis of proteome-metabolome interaction combined with targeted**  
4 **transcriptomics allowed a deeper characterization of the bud**  
5 353 **differentiation process**  
6 354

7  
8 355 The integration of metabolome and proteome datasets also allowed the definition of a protein-  
9 356 metabolite interaction network based on the different correlations between variables of different  
10 357 types. The resulting network (Figure 4; correlation >0.75) showed two interaction clusters. First  
11 358 cluster (Figure 4A, left) gathered proteins and metabolites more abundant in the apical sections  
12 359 of [juvenileyoung](#) buds (Figures 4B-D). Proteins in this cluster are related to protein biosynthesis  
13 360 and transport (ribosomal-related, CHAPERONIN TCP1, TMP21), transcriptional response to  
14 361 stress (GERMIN, NUCLEIC ACID BINDING PROTEIN), and a PHOSPHOESTERASE similar to  
15 362 Arabidopsis PURPLE ACID PHOSPHATASE, PAP14 (At2g46880), required for petal  
16 363 differentiation and expansion (Zhu et al., 2005). These proteins positively correlated to different  
17 364 terpenoids (mascaroside, loganin, menthane) and the flavonoid luteolin. The abundance of these  
18 365 variables greatly diminished during the transition to basal section and also in [adultmature](#) buds.  
19 366 4,4'-ditolylthiourea, the only metabolite in this cluster whose abundance is maximal in the basal  
20 367 section of [adultmature](#) buds, showed negative correlations to all of its linked nodes.

21 368 Second cluster (Figure 4A, right) was not as selective in its variable categories as first cluster,  
22 369 since groups variables peaking at each developmental stage and bud section. However, there  
23 370 was a major presence of variables more accumulated in [adultmature](#) tissues and/or basal sections  
24 371 of the buds (Figures 4C, D). [JuvenileYoung](#) buds are characterized by an increased  
25 372 photosynthesis (active center of PSII, GAPDH) and glycolytic (PYRUVATE KINASE,  
26 373 PHOSPHOFRUCTOKINASE) pathways. HISTONE H4, GDSL ESTERASE LIPASE, and  
27 374 elements related to protein biosynthesis (eRF1, protease inhibitor SERPIN, ribosomal proteins  
28 375 L15 and L50) and redox (THIOREDOXIN, START-like domain protein) were also more abundant  
29 376 in [juvenileyoung](#) buds. Most of these enzymes were positively correlated to N1751, an unknown  
30 377 metabolite, and were characteristic of basal sections of the bud. On the other hand, [adultmature](#)  
31 378 buds had increased energetic (fructose-6-P and ATPase), signaling and gene regulation (14-3-3  
32 379 protein gamma, HISTONE H3, regulator of ribonuclease activity), antioxidant/detoxification  
33 380 activities (dihydrolipoate), and proteome remodeling (ribosomal proteins and peptidases). 2-  
34 381 alpha-(S)-Strictosidine, a key compound in monoterpene indol alkaloyds biosynthetic pathway  
35 382 (Rüffer et al., 1978), was mostly accumulated in the basal sections.

36 383 Interestingly, HISTONE H3, and other proteins related to epigenetic regulation of gene expression  
37 384 formed a cluster that had a greater accumulation in [adultmature](#) buds. Despite having a positive  
38 385 correlation to most of the metabolites of this cluster, it negatively correlated to those metabolites  
39 386 accumulated in [juvenileyoung](#) buds. HISTONE H4, characteristic of [juvenileyoung](#) tissues,  
40 387 negatively correlated to metabolite P0265 and through it to glycolytic and carbon-related  
41 388 enzymes, suggesting its role in regulation of energetic pathways. Finally, 14-3-3 Protein gamma,  
42 389 involved in the signaling pathways of the main plant hormones (Camoni et al., 2018), was also  
43 390 accumulated in [adultmature](#) buds in the apical section. However, in this case, it was negatively

391 correlated to most of the metabolites in this cluster, some of them as relevant as diphyllin, lignin  
392 (Hemmati et al., 2007), or fructose-6-P.

393 In order to support hypotheses raised after proteometabolomic dataset, six genes related to the  
394 different activities of the clusters depicted above were analyzed by qPCR (Figure 5). According  
395 to transcriptomics results, the different treatment had different expression patterns of the analyzed  
396 genes. Apical section of [juvenileyoung](#) buds had a differential overexpression of  
397 *ADENOSYLHOMOCYSTEINASE (SAHH)*, related to epigenetic regulation (Tanaka et al., 1997;  
398 Rocha et al., 2005), and *GLUTATHIONE S-TRANSFERASE (GST)* and *PHENYLALANINE*  
399 *AMMONIA LYASE (PAL)*, both genes involved in secondary metabolism and hormonal signaling  
400 (Hahlbrock and Scheel, 1989; Rivero et al., 2001; Dixon et al., 2010; Czerniawski and Bednarek,  
401 2018). The expression level of these genes was similar in [adultmature](#) buds and in the basal part  
402 of the [juvenileyoung](#) bud.

403 *S-ADENOSYLMETHIONINE SYNTHASE (SAM SYNTHASE)*, a central element in DNA  
404 methylation (Gómez-Gómez and Carrasco, 1998) was more expressed in [juvenileyoung](#) buds, as  
405 *NEDD8-ACTIVATING ENZYME E1 CATALYTIC SUBUNIT (NEDD8-E1)*, involved in proteome  
406 remodelling and DNA repair (Brown and Jackson, 2015; Brown et al., 2015). Finally, it is important  
407 to highlight the expression pattern of the *MORE AXILLARY GROWTH 1 (MAX1)* gene, which is  
408 required for hormonal biosynthesis of a shoot-branching inhibiting signal (Booker et al., 2005).  
409 *MAX1* increased its expression in [juvenileyoung](#) basal section, while its expression decreased  
410 drastically in [adultmature](#) basal section.

## 411 412 **DISCUSSION**

413 The study of the transition between [juvenileyoung](#) and [adultmature](#) buds, and how it is reflected  
414 at metabolome and proteome levels, is not only crucial in order to understand shoot growth and  
415 tree architecture, but also to improve relevant traits for forestry such as total growth or polycyclism  
416 (Cabezas et al., 2015). Growth-related traits are influenced not only by their inherent genetic  
417 factors (most of them polygenic) but also by the environment (Zas and Fernández-López, 2005).  
418 Environmental conditions (light, temperature, rainfall) in combination with the genotype define not  
419 only the yearly tree growth period, ontogenic stage and flowering time, but also tree architecture,  
420 modulating for instance, polycyclism (Meijón et al., 2016; de Simón et al., 2018). The combination  
421 of genetic and environmental factors, together with the different growth patterns of mature and  
422 [juvenileyoung](#) buds sometimes mixed in trees of the same age, makes the apical growth in *Pinus*  
423 *pinaster* very complex at physiological and molecular levels (Nguyen et al., 1995). Consequently,  
424 the characterization of the proteome and metabolome of buds in different developmental stages  
425 is a necessary first step towards the fully understanding of all of these processes.

426 The employment of an integrative approach allowed the characterization of bud maturation from  
427 a holistic perspective, identifying the key molecular pathways of this process. Two main sources  
428 of variation were clearly distinguished after clustering and multivariate analyses. The first was the  
429 bud maturation status ([juvenileyoung](#) vs [adultmature](#)) and the second the presence of apical or

1  
2  
3 430 lateral meristems (apical vs basal section of the buds), each of them with a different set of  
4 431 characteristic biomolecules.

5  
6 432 [AdultMature](#) buds exhibit specific phenology and growth patterns distinct from [juvenileyoung](#)  
7 433 buds. In the [juvenileyoung](#) stage, leaf primordia differentiate into photosynthetically active primary  
8 434 needles. Axillary buds develop either into auxiblasts in basal positions or into randomly distributed  
9 435 brachyblasts in more distal positions on the stem. When trees reach the [adultmature](#) stage, leaf  
10 436 primordia differentiate into scale leaves, and photosynthetic activity is shifted to long needles  
11 437 differentiated on brachyblasts (Nguyen et al., 1995; Jordy, 2004). The physiological competence  
12 438 of [adultmature](#) buds was probably imposed by the increased abundance of ABA and specific  
13 439 gibberelins (bioactive GA1 and intermediary GA19; Supplementary Table S3). ABA has not only  
14 440 a role in dormancy, but also in dormancy release and bud set in combination with specific  
15 441 gibberellins (Zheng et al., 2015; Maurya et al., 2018; Vimont et al., 2019). Interestingly,  
16 442 [juvenileyoung](#) buds had slightly lower concentrations of ABA but an increased abundance of  
17 443 bioactive GA3, and GA8, a degradation product of GA1. Both gibberellins, GA1 and GA3, are  
18 444 related to shoot elongation (Little and MacDonald, 2003); however, is complicated to venture  
19 445 which specific role are playing each one in the different development stage of the bud.  
20 446 Additionally, in relation to hormonal signaling, a key element was identified in the network, 14-3-  
21 447 3 protein. A possible role for 14-3-3 proteins in the coordination of GA and ABA signaling has  
22 448 emerged in the last years (Cameni et al., 2018). In fact, the overexpression of ABA responsive,  
23 449 14-3-3-interacting transcription factors ABF1-3 impairs GA action, indicating that they act as  
24 450 negative regulators of GA signaling and that 14-3-3 proteins may function by sequestering ABF1-3  
25 451 in the cytoplasm. However, the mechanism of 14-3-3 action and all the elements involved in the  
26 452 ABA and GA coordination are still unknown.

27  
28 453 As pointed by datasets and correlation networks, having the enzymatic machinery to increase  
29 454 metabolic rate allowing burst and growth seems to be essential in [juvenileyoung](#) buds, since  
30 455 enzymes of photosynthesis and glycolytic pathways were increased compared to [adultmature](#)  
31 456 (Figures 2 and 4). Interestingly, the accumulation of fructose-6-P in [adultmature](#) buds indicate not  
32 457 only a differential allocation of sugars between ontogenic stages, but also specific hormonal,  
33 458 growth (Eveland and Jackson, 2012), and maturation patterns (Uggla et al., 2001). Lipids such  
34 459 as pimelate and dihydroxylipoate with a dual redox and transcriptional regulation role (Sen and  
35 460 Packer, 1996) were also accumulated in [adultmature](#) buds. The mature secondary metabolism  
36 461 was also reflected by the accumulation of flavonoids. Flavonoids and tannins may be involved in  
37 462 cellular detoxification (Meijón et al., 2016) and also in plant resistance against herbivores or other  
38 463 stresses (Treutter, 2008). At the end of the growing season, accumulation of lipid and starch is  
39 464 positively correlated with the onset of dormancy in [adultmature](#) buds (Jordy, 2004). Bud  
40 465 development is also associated to different abiotic stress tolerance and proteins related to  
41 466 detoxification. In all analyzed tissues, there were a great abundance of heat shock or chaperonin-  
42 467 like proteins (TCP1, CPN10) and ROS detoxifying enzymes (peroxidases, thioredoxines);  
43 468 however, mature buds were characterized by higher abundances of these protein families,

1  
2  
3 469 suggesting that the greater tolerance to stress exhibited by these buds (Miller et al., 2008) relies  
4 470 on the overaccumulation of these [mechanismsmolecules](#), compared to [juvenileyoung](#) tissues.

5  
6 471 The different cell competence is defined by specific protein sets consequence of differential  
7  
8 472 transcriptional and post-transcriptional regulation (del Mar Castellano et al., 2004; Dembinsky et  
9  
10 473 al., 2007). [AdultMature](#) and [juvenileyoung](#) buds have a differential set of DNA/RNA interacting  
11 474 proteins and ribosomal proteins. Among them, START-like domain proteins were up-accumulated  
12 475 in [juvenileyoung](#) tissues, despite one characteristic of [adultmature](#) buds (PPI00057470). The  
13 476 specific dynamic of this family, which is required for regulating transcription factors needed for  
14 477 cell differentiation after binding a lipid ligand (Schrick et al., 2014; Grabon et al., 2019), illustrates  
15 478 the complexity of bud maturation. [JuvenileYoung](#) buds were characterized by the serin protease  
16 479 inhibitors SERPIN (+5-fold change compared to [adultmature](#)) (Supplementary Table S2), which  
17 480 has been proposed to have also a non-peptidase inhibitory functions negatively regulating stress-  
18 481 induced cell death or reducing gene expression by compacting chromatin (Cohen et al., 2019).  
19 482 Epigenetic regulation elements were also differential between [adultmature](#) and [juvenileyoung](#)  
20 483 buds (discussed below).

21  
22 484 The complexity of a pine bud was also reflected in the direct comparison of its apical and basal  
23 485 sections. The former containing the shoot apical meristem, and the later the lateral meristems  
24 486 and needle primordia (Fernando, 2014). This organization implies physiological and metabolic  
25 487 differences, which has been validated through this work. Starch, lipid reserves, and tannins are  
26 488 known to accumulate in the shoot tip as pines become older (Jordy et al., 2000; Jordy, 2004). The  
27 489 accumulation of flavonoids and its biosynthetic machinery in the apical part of the buds reinforces  
28 490 its role in the protection of the meristem (Meijón et al., 2016) and also in the vegetative bud  
29 491 outgrowth. Differential organogenetic activity in apical and basal sections, changeable across the  
30 492 bud maturation, is also related to environment conditions and apical dominance regulation (Jordy,  
31 493 2004; Hover et al., 2017). Thus, the high activity of *MAX1* gene in both sections of [juvenileyoung](#)  
32 494 bud suggests the essential role of strigolactone hormone regulating inhibition of axillary bud  
33 495 outgrowth in this phase; however, in mature bud, *MAX1* expression is higher in apical section  
34 496 (Figure 5). The current models in relation to control of apical dominance suggest complex  
35 497 interaction networks where sugars and ABA could be responsible for initial release of an apical  
36 498 bud, while auxins, strigolactones and cytokinins seem to determine sustained outgrowth of axillary  
37 499 buds (Nguyen and Emery, 2017). Gibberellins, despite being their role well known in shoot  
38 500 elongation, need more investigation to determine their function inside this network. However,  
39 501 some reports on their interaction with strigolactone suggest that increased gibberellin levels could  
40 502 repress axillary bud outgrowth (Luisi et al., 2011).

41  
42 503 The basal part of the bud is prepared to burst, contrary to apical whose function is keeping and  
43 504 protecting apical meristem, and many cell division and development-related proteins like FTSZ  
44 505 needed for plastid division (Schmitz et al., 2009), dormancy/associated or DNA repair machinery  
45 506 (Os08g0519400 like protein) were up-accumulated. LEA proteins and TMP21, associated to less  
46 507 differentiated organs (Zimmerman, 1993), were characteristic of the apical part of the buds  
47  
48  
49  
50  
51  
52  
53  
54  
55  
56  
57  
58  
59  
60

508 probably helping to maintain meristem identity together with specific abundances of growth  
509 regulators and nucleic acid binding proteins and histone modifications regulating gene  
510 expression.

511 The great amount of differential proteins and metabolites involved in epigenetic regulation  
512 suggests the key role of these mechanisms in bud development. DNA methylation is a well-known  
513 epigenetic mark of transcriptional gene silencing, but also in the establishment of  
514 heterochromatin, transposon control and genomic imprinting (Galindo-González et al., 2018).  
515 Two of the key enzymes regulating the methylation cycle, SAM SYNTHASE and SAHH, showed  
516 an overaccumulation in [juvenileyoung](#) buds and more specifically in its apical part (Figure 5),  
517 suggesting that bud maturation is concomitant to increased DNA methylation levels as previously  
518 reported in *Pinus radiata* (Fraga et al., 2002). ARGONAUTE, a key enzyme involved in RNA-  
519 mediated DNA methylation, was overaccumulated in [adultmature](#) apical buds, which will be  
520 probably related to the hypermethylation associated to development. Despite the employed  
521 analytical procedures were not intended to describe post-translational modifications defining  
522 histone code, specific forms of HISTONE H3 and H4 were characteristic of each developmental  
523 stage, reinforcing the hypothesis that bud maturation is the consequence of a complex interaction  
524 between epigenetic mechanisms, transcription factors and hormonal regulators.

525 Overall, our study provided novel insights over bud maturation and the machinery involved in its  
526 development and growth and stress resilience at different molecular levels and pathways. The  
527 comprehensive overview of this process allowed the validation of proteins and metabolites  
528 involved in bud development that were previously described, but also the involvement of novel  
529 proteins, metabolites, and pathways. However, further studies will be necessary to validate these  
530 new set of candidate molecules by using buds coming from different populations that show  
531 [contrastant contrasting](#) wood quality and stress tolerance.

532

## 533 DATA AND MATERIALS AVAILABILITY

534 All relevant data can be found within the manuscript and supplementary materials.

535

## 536 SUPPLEMENTARY MATERIAL

537 **Table S1.** Genes and primers employed in quantitative PCR analyses.

538 **Table S2.** Proteins identification according to SEQUEST (scores, % of coverage, number of  
539 common, unique, and razor peptides), quantification (mean  $\pm$  SD of three biological replicates),  
540 univariate analysis (p and q values; TukeyHSD p values for all paired comparisons).

541 **Table S3.** Peaks obtained after UPLC-MS analysis of polar metabolites. Peaks were aligned with  
542 mzMine 2.10 avoiding redundancies between positive (P) and negative (N) modes. This table  
543 shows peak ID, adduct, m/z, retention time, normalized peak areas for each analyzed sample,  
544 and univariate analysis (p and q values; TukeyHSD p values for all paired comparisons). Peak  
545 compound description is provided according to Supplementary Table S4.

1  
2  
3 546 **Table S4.** Identification of metabolites in the 3670 peaks that were analyzed. a) 133 peaks were  
4 547 unequivocally identified (those metabolites that were defined after the comparison to our  
5 548 compound library or by comparison of the MS/MS to *online* databases). b) 987 peaks were  
6 549 tentatively assigned after comparing its very accurate mass to reference compound databases.  
7 550 Delta ppm and compound exact mass are provided. Annotation source, molecular form, and  
8 551 accessions of KEGG, FooDB and other databases are provided for all identified/assigned  
9 552 compounds.

10 553 **Table S5.** DIABLO integrative analysis of proteome and metabolome datasets. a) Sample scores  
11 554 for components 1 and 2 in both datasets, b) variance explained for each component, and c)  
12 555 variable loadings for both datasets.

13 556 **Figure S1.** Integrative clustering of proteome and metabolome analysis (High resolution Figure  
14 557 3B).

15 558

## 16 559 **DISCLOSURES**

17 560 The authors have no conflicts of interest to declare.

18 561

## 19 562 **FUNDING**

20 563 This publication is an output of the National Project Vampiro (AGL2017-83988-R, Spanish  
21 564 Ministry of Economy and Competitiveness). M.M. and L.V. were supported by Ramón y Cajal  
22 565 program (RYC-2014-14981 and RYC-2015-17871, respectively; Spanish Ministry of Economy  
23 566 and Competitiveness). L.G.C and S.G. were supported by Severo Ochoa Predoctoral Program  
24 567 (BP19-146 and BP19-145, respectively; Principality of Asturias, Spain).

25 568

## 26 569 **ACKNOWLEDGMENTS**

27 570 The authors wish to thank Eloy A. Ron (SERPA S.A, Vivero Forestal de La Mata,) for providing  
28 571 the *Pinus pinaster* seedlings employed in this work.

29 572

## 30 573 **AUTHORS' CONTRIBUTIONS**

31 574 MM and LV designed the experiments, performed mass-spectrometry analyses, and  
32 575 metabolome-related computational analysis. LV and SG performed proteome-related  
33 576 computational analysis. LGC performed targeted-transcriptomics analyses. LV and SG performed  
34 577 statistical analyses. All authors wrote the manuscript, read, and approved the final version of the  
35 578 manuscript.

36 579



580

## 581 REFERENCES

582

583

584

585

586

587

588

589

590

591

592

593

594

595

596

597

598

599

600

601

602

603

604

605

606

607

608

609

610

611

612

613

614

615

616

617

618

619

620

621

622

623

624

625

626

627

628

629

630

631

632

633

634

635

636

637

- Allenbach, L., and Poirier, Y. (2000). Analysis of the alternative pathways for the  $\beta$ -oxidation of unsaturated fatty acids using transgenic plants synthesizing polyhydroxyalkanoates in peroxisomes. *Plant Physiol.* 124, 1159-1168. doi: 10.1104/pp.124.3.1159
- Allona, I., Quinn, M., Shoop, E., Swope, K., Cyr, S.S., Carlis, J., et al. (1998). Analysis of xylem formation in pine by cDNA sequencing. *Proc. Natl. Acad. Sci. U.S.A.* 95, 9693-9698. doi: 10.1073/pnas.95.16.9693
- Alonso, P., Cortizo, M., Cantón, F.R., Fernández, B., Rodríguez, A., Centeno, M.L., et al. (2007). Identification of genes differentially expressed during adventitious shoot induction in *Pinus pinea* cotyledons by subtractive hybridization and quantitative PCR. *Tree Physiol.* 27, 1721-1730. doi: 10.1093/treephys/27.12.1721
- Baldermann, S., Homann, T., Neugart, S., Chmielewski, F.-M., Götz, K.-P., Gödeke, K., et al. (2018). Selected plant metabolites involved in oxidation-reduction processes during bud dormancy and ontogenetic development in sweet cherry buds (*Prunus avium* L.). *Molecules* 23, 1197. doi: 10.3390/molecules23051197
- Booker, J., Sieberer, T., Wright, W., Williamson, L., Willett, B., Stirnberg, P., et al. (2005). *MAX1* encodes a cytochrome P450 family member that acts downstream of *MAX3/4* to produce a carotenoid-derived branch-inhibiting hormone. *Dev. Cell.* 8, 443-449. doi: 10.1016/j.devcel.2005.01.009
- Bräutigam, K., Vining, K.J., Lafon-Placette, C., Fossdal, C.G., Mirouze, M., Marcos, J.G., et al. (2013). Epigenetic regulation of adaptive responses of forest tree species to the environment. *Ecol. Evol.* 3, 399-415. doi: 10.1002/ece3.461
- Brown, J.S., and Jackson, S.P. (2015). Ubiquitylation, neddylation and the DNA damage response. *Open Biol.* 5, 150018. doi: 10.1098/rsob.150018
- Brown, J.S., Lukashchuk, N., Sczaniecka-Clift, M., Britton, S., le Sage, C., Calsou, P., et al. (2015). Neddylation promotes ubiquitylation and release of Ku from DNA-damage sites. *Cell Rep.* 11, 704-714. doi: 10.1016/j.celrep.2015.03.058
- Brunner, A.M., Varkonyi-Gasic, E., and Jones, R.C. (2017). "Phase change and phenology in trees," in *Comparative and evolutionary genomics of angiosperm trees*, eds A. T. Groover and Q. C. B. Cronk (Cham: Springer International Publishing AG), 227-274.
- Byrne, M.E. (2009). A role for the ribosome in development. *Trends Plant Sci.* 14, 512-519. doi: 10.1016/j.tplants.2009.06.009
- Cabezas, J.A., González-Martínez, S.C., Collada, C., Guevara, M.A., Boury, C., de María, N., et al. (2015). Nucleotide polymorphisms in a pine ortholog of the Arabidopsis degrading enzyme cellulase KORRIGAN are associated with early growth performance in *Pinus pinaster*. *Tree Physiol.* 35, 1000-1006. doi: 10.1093/treephys/tpv050
- Camoni, L., Visconti, S., Aducci, P., and Marra, M. (2018). 14-3-3 proteins in plant hormone signaling: doing several things at once. *Front. Plant Sci.* 9, 297. doi: 10.3389/fpls.2018.00297
- Canales, J., Bautista, R., Label, P., Gómez-Maldonado, J., Lesur, I., Fernández-Pozo, N., et al. (2014). De novo assembly of maritime pine transcriptome: implications for forest breeding and biotechnology. *Plant Biotechnol. J.* 12, 286-299. doi: 10.1111/pbi.12136
- Cano, M., Morcillo, A., Humánez, A., Mendoza-Poudereux, I., Alborch, A., Segura, J., et al. (2018). "Maritime Pine (*Pinus Pinaster* Aiton)," in *Step Wise Protocols for Somatic Embryogenesis of Important Woody Plants: Volume I Forestry Sciences 84*, eds S. M. Jain and P. Gupta (Cham: Springer International Publishing AG), 167-179.
- Cañas, R.A., Canales, J., Muñoz-Hernández, C., Granados, J.M., Ávila, C., García-Martín, M.L., et al. (2015). Understanding developmental and adaptive cues in pine through metabolite profiling and co-expression network analysis. *J. Exp. Bot.* 66, 3113-3127. doi: 10.1093/jxb/erv118
- Chen, J.C., Jiang, C.Z., and Reid, M.S. (2005). Silencing a prohibitin alters plant development and senescence. *Plant J.* 44, 16-24. doi: 10.1111/j.1365-3113X.2005.02505.x
- Chepyshko, H., Lai, C.-P., Huang, L.-M., Liu, J.-H., and Shaw, J.-F. (2012). Multifunctionality and diversity of GDSL esterase/lipase gene family in rice (*Oryza sativa* L. *japonica*) genome: new insights from bioinformatics analysis. *BMC Genomics.* 13, 309. doi: 10.1186/1471-2164-13-309

- 1  
2  
3 638 Cohen, M., Davydov, O., and Fluhr, R. (2019). Plant serpin protease inhibitors: specificity and  
4 639 duality of function. *J. Exp. Bot.* 70, 2077-2085. doi: 10.1093/jxb/ery460
- 5 640 Conde, D., Moreno-Cortés, A., Dervinis, C., Ramos-Sánchez, J.M., Kirst, M., Perales, M., et al.  
6 641 (2017). Overexpression of DEMETER, a DNA demethylase, promotes early apical bud  
7 642 maturation in poplar. *Plant Cell Environ.* 40, 2806-2819. doi: 10.1111/pce.13056
- 8 643 Czerniawski, P., and Bednarek, P. (2018). Glutathione S-transferases in the biosynthesis of  
9 644 sulfur-containing secondary metabolites in Brassicaceae plants. *Front. Plant Sci.* 9, 1639.  
10 645 doi: 10.3389/fpls.2018.01639
- 11 646 Das, A., Paudel, B., and Rohila, J.S. (2015). "Potentials of proteomics in crop breeding," in  
12 647 *Advances in plant breeding strategies: breeding, biotechnology and molecular tools*, eds  
13 648 J. M. Al-Khayri, S. M. Jain and D. V. Johnson (Cham: Springer International Publishing  
14 649 AG), 513-537.
- 15 650 De Simón, B.F., Cadahía, E., and Aranda, I. (2018). Metabolic response to elevated CO<sub>2</sub> levels  
16 651 in *Pinus pinaster* Aiton needles in an ontogenetic and genotypic-dependent way. *Plant*  
17 652 *Physiol. Biochem.* 132, 202-212. doi: 10.1016/j.plaphy.2018.09.006
- 18 653 De Simón, B.F., Sanz, M., Cervera, M.T., Pinto, E., Aranda, I., and Cadahía, E. (2017). Leaf  
19 654 metabolic response to water deficit in *Pinus pinaster* Ait. relies upon ontogeny and  
20 655 genotype. *Environ. Exp. Bot.* 140, 41-55. doi: 10.1016/j.envexpbot.2017.05.017
- 21 656 Del Mar Castellano, M., Boniotti, M.B., Caro, E., Schnittger, A., and Gutierrez, C. (2004). DNA  
22 657 replication licensing affects cell proliferation or endoreplication in a cell type-specific  
23 658 manner. *Plant Cell* 16, 2380-2393. doi: 10.1105/tpc.104.022400
- 24 659 Dembinsky, D., Woll, K., Saleem, M., Liu, Y., Fu, Y., Borsuk, L.A., et al. (2007). Transcriptomic  
25 660 and proteomic analyses of pericycle cells of the maize primary root. *Plant Physiol.* 145,  
26 661 575-588. doi: 10.1104/pp.107.106203
- 27 662 Dixon, D.P., Skipsey, M., and Edwards, R. (2010). Roles for glutathione transferases in plant  
28 663 secondary metabolism. *Phytochemistry* 71, 338-350. doi:  
29 664 10.1016/j.phytochem.2009.12.012
- 30 665 Escandón, M., Valledor, L., Pascual, J., Pinto, G., Cañal, M.J., and Meijón, M. (2017). System-  
31 666 wide analysis of short-term response to high temperature in *Pinus radiata*. *J. Exp. Bot.*  
32 667 68, 3629-3641. doi: 10.1093/jxb/erx198
- 33 668 Eveland, A.L., and Jackson, D.P. (2012). Sugars, signalling, and plant development. *J. Exp. Bot.*  
34 669 63, 3367-3377. doi: 10.1093/jxb/err379
- 35 670 FAO (2009). *Global demand for wood products. Rome: Italy: The Food and Agricultural*  
36 671 *Organization of the United Nations.* Available at:  
37 672 <http://www.fao.org/3/i0350e/i0350e00.htm>
- 38 673 FAO (2015). *Global forest resources assessment 2015. Rome, Italy.* FAO Forestry Paper No. 1.  
39 674 Available at: [http://www.fao.org/forest-resources-assessment/past-assessments/fra-](http://www.fao.org/forest-resources-assessment/past-assessments/fra-2015/en/)  
40 675 [2015/en/](http://www.fao.org/forest-resources-assessment/past-assessments/fra-2015/en/)
- 41 676 Fernández, H., Fraga, M., Bernard, P., and Revilla, M. (2003). Quantification of GA1, GA3, GA4,  
42 677 GA7, GA9, and GA20 in vegetative and male cone buds from juvenile and mature trees  
43 678 of *Pinus radiata*. *Plant Growth Regul.* 40, 185-188. doi: 10.1023/A:1025070707899
- 44 679 Fernando, D.D. (2014). The pine reproductive process in temperate and tropical regions. *New*  
45 680 *For.* 45, 333-352. doi: 10.1007/s11056-013-9403-7
- 46 681 Fraga, M.F., Rodríguez, R., and Cañal, M.J. (2002). Genomic DNA methylation-demethylation  
47 682 during aging and reinvigoration of *Pinus radiata*. *Tree Physiol.* 22, 813-816. doi:  
48 683 10.1093/treephys/22.11.813
- 49 684 Galindo-González, L., Sarmiento, F., and Quimbaya, M.A. (2018). Shaping plant adaptability,  
50 685 genome structure and gene expression through transposable element epigenetic control:  
51 686 Focus on methylation. *Agronomy* 8, 180. doi: 10.3390/agronomy8090180
- 52 687 Garcés, M., Le Provost, G., Lalanne, C., Claverol, S., Barré, A., Plomion, C., et al. (2014).  
53 688 Proteomic analysis during ontogenesis of secondary xylem in maritime pine. *Tree*  
54 689 *Physiol.* 34, 1263-1277. doi: 10.1093/treephys/tp117
- 55 690 Girard, F., Vennetier, M., Ouarmim, S., Caraglio, Y., and Misson, L. (2011). Polycyclism, a  
56 691 fundamental tree growth process, decline with recent climate change: the example of  
57 692 *Pinus halepensis* Mill. in Mediterranean France. *Trees Struct. Funct.* 25, 311-322. doi:  
58 693 10.1007/s00468-010-0507-9
- 59 694 Gómez-Gómez, L., and Carrasco, P. (1998). Differential expression of the S-Adenosyl-L-  
60 695 Methionine Synthase genes during pea development. *Plant Physiol.* 117, 397-405. doi:  
61 696 10.1104/pp.117.2.397

- 1  
2  
3 697 González, Á.C., Díaz, I.F., de la Torre, C., Vázquez, J.P., Colina, F.J., Villedor, L., et al. (2016).  
4 698 Nuevos marcadores de calidad de madera en *Pinus pinaster*: Estrigolactonas y  
5 699 ramificación. *Tecnología agroalimentaria: Boletín informativo del SERIDA* 17, 21-27.  
6 700 Grabon, A., Bankaitis, V.A., and McDermott, M.I. (2019). The interface between  
7 701 phosphatidylinositol transfer protein function and phosphoinositide signaling in higher  
8 702 eukaryotes. *J. Lipid Res.* 60, 242-268. doi: 10.1194/jlr.R089730  
9 703 Großskinsky, D.K., Syaifullah, S.J., and Roitsch, T. (2017). Integration of multi-omics techniques  
10 704 and physiological phenotyping within a holistic phenomics approach to study senescence  
11 705 in model and crop plants. *J. Exp. Bot.* 69, 825-844. doi: 10.1093/jxb/erx333  
12 706 Haffner, V., Enjalric, F., Lardet, L., and Carron, M. (1991). Maturation of woody plants: a review  
13 707 of metabolic and genomic aspects. *Ann. For. Sci.* 48, 615-630. doi:  
14 708 10.1051/forest:19910601  
15 709 Hahlbrock, K., and Scheel, D. (1989). Physiology and molecular biology of phenylpropanoid  
16 710 metabolism. *Annu. Rev. Plant Biol. Plant. Mol. Biol.* 40, 347-369. doi:  
17 711 10.1146/annurev.pp.40.060189.002023  
18 712 Harwood, J.L. (1996). Recent advances in the biosynthesis of plant fatty acids. *Biochim. Biophys.*  
19 713 *Acta* 1301, 7-56. doi: 10.1016/0005-2760(95)00242-1  
20 714 Hemmati, S., Schneider, B., Schmidt, T.J., Federolf, K., Alfermann, A.W., and Fuss, E. (2007).  
21 715 Justicidin B 7-hydroxylase, a cytochrome P450 monooxygenase from cell cultures of  
22 716 *Linum perenne* Himmelszelt involved in the biosynthesis of diphyllin. *Phytochemistry* 68,  
23 717 2736-2743. doi: 10.1016/j.phytochem.2007.10.025  
24 718 Hover, A., Buissart, F., Caraglio, Y., Heinz, C., Pailler, F., Ramel, M., et al. (2017). Growth  
25 719 phenology in *Pinus halepensis* Mill.: apical shoot bud content and shoot elongation. *Ann.*  
26 720 *For. Sci.* 74, 39. doi: 10.1007/s13595-017-0637-y  
27 721 Considine, M.J., and Foyer, C.H. (2014). Redox Regulation of Plant Development. *Antioxid.*  
28 722 *Redox Signal.* 21, 1305-1326. doi: 10.1089/ars.2013.5665  
29 723 Jordy, M.-N., Danti, S., Favre, J.-M., and Raccchi, M.L. (2000). Histological and biochemical  
30 724 changes in *Pinus* spp. seeds during germination and post-germinative growth:  
31 725 triacylglycerol distribution and catalase activity. *Aust. J. Plant Physiol.* 27, 1109-1117. doi:  
32 726 10.1071/PP00069  
33 727 Jordy, M.N. (2004). Seasonal variation of organogenetic activity and reserves allocation in the  
34 728 shoot apex of *Pinus pinaster* Ait. *Ann. Bot.* 93, 25-37. doi: 10.1093/aob/mch005  
35 729 Kamada, I., Yamauchi, S., Youssefian, S., and Sano, H. (1992). Transgenic tobacco plants  
36 730 expressing *rgp1*, a gene encoding a RAS-related GTP-binding protein from rice, show  
37 731 distinct morphological characteristics. *Plant J.* 2, 799-807. doi: 10.1111/j.1365-  
38 732 313X.1992.tb00149.x  
39 733 Kim, D., Shin, H., Song, Y.S., and Kim, J.H. (2012). Synergistic effect of different levels of genomic  
40 734 data for cancer clinical outcome prediction. *J. Biomed. Inform.* 45, 1191-1198. doi:  
41 735 10.1016/j.jbi.2012.07.008  
42 736 Little, C., and MacDonald, J.E. (2003). Effects of exogenous gibberellin and auxin on shoot  
43 737 elongation and vegetative bud development in seedlings of *Pinus sylvestris* and *Picea*  
44 738 *glauca*. *Tree Physiol.* 23, 73-83. doi: 10.1093/treephys/23.2.73  
45 739 Lohse, M., Nagel, A., Herter, T., May, P., Schroda, M., Zrenner, R., et al. (2014). Mercator: a fast  
46 740 and simple web server for genome scale functional annotation of plant sequence data.  
47 741 *Plant Cell Environ.* 37, 1250-1258. doi: 10.1111/pce.12231  
48 742 López-Goldar, X., Villari, C., Bonello, P., Borg-Karlson, A.K., Grivet, D., Sampedro, L., et al.  
49 743 (2019). Genetic variation in the constitutive defensive metabolome and its inducibility are  
50 744 geographically structured and largely determined by demographic processes in maritime  
51 745 pine. *J. Ecol.* 107, 2464-2477. doi: 10.1111/1365-2745.13159  
52 746 López-Goldar, X., Zas, R., Sampedro, L. (2020). Resource availability drives microevolutionary  
53 747 patterns of plant defences. *Funct. Ecol.*, 1-13. doi: 10.1111/1365-2435.13610  
54 748 Luisi, A., Lorenzi, R., and Sorce, C. (2011). Strigolactone may interact with gibberellin to control  
55 749 apical dominance in pea (*Pisum sativum*). *Plant Growth Regul.* 65, 415-419. doi:  
56 750 10.1007/s10725-011-9603-0  
57 751 Maurya, J.P., Triozzi, P.M., Bhalerao, R.P., and Perales, M. (2018). Environmentally sensitive  
58 752 molecular switches drive poplar phenology. *Front. Plant Sci.* 9, 1873. doi:  
59 753 10.3389/fpls.2018.01873  
60 754 Meijón, M., Feito, I., Oravec, M., Delatorre, C., Weckwerth, W., Majada, J., et al. (2016). Exploring  
61 755 natural variation of *Pinus pinaster* Aiton using metabolomics: Is it possible to identify the

- 1  
2  
3 756 region of origin of a pine from its metabolites? *Mol. Ecol.* 25, 959-976. doi:  
4 757 10.1111/mec.13525
- 5 758 Meijón, M., Rodríguez, R., Cañal, M.J., and Feito, I. (2009). Improvement of compactness and  
6 759 floral quality in azalea by means of application of plant growth regulators. *Sci. Hortic-  
7 760 Amsterdam* 119, 169-176. doi: 10.1016/j.scienta.2008.07.023
- 8 761 Miller, G., Shulaev, V., and Mittler, R. (2008). Reactive oxygen signaling and abiotic stress.  
9 762 *Physiol. Plantarum* 133, 481-489. doi: 10.1111/j.1399-3054.2008.01090.x
- 10 763 Mochida, K., and Shinozaki, K. (2011). Advances in omics and bioinformatics tools for systems  
11 764 analyses of plant functions. *Plant Cell Physiol.* 52, 2017-2038. doi: 10.1093/pcp/pcr153
- 12 765 Moon, J., Parry, G., and Estelle, M. (2004). The ubiquitin-proteasome pathway and plant  
13 766 development. *Plant Cell* 16, 3181-3195. doi: 10.1105/tpc.104.161220
- 14 767 Morel, A., Trontin, J.-F., Corbineau, F., Lomenech, A.-M., Beaufour, M., Reymond, I., et al. (2014).  
15 768 Cotyledonary somatic embryos of *Pinus pinaster* Ait. most closely resemble fresh,  
16 769 maturing cotyledonary zygotic embryos: biological, carbohydrate and proteomic  
17 770 analyses. *Planta* 240, 1075-1095. doi: 10.1007/s00425-014-2125-z
- 18 771 Morisseau, C. (2013). Role of epoxide hydrolases in lipid metabolism. *Biochimie* 95, 91-95. doi:  
19 772 10.1016/j.biochi.2012.06.011
- 20 773 Nguyen, A., Dormling, I., and Kremer, A. (1995). Characterization of *Pinus pinaster* seedling  
21 774 growth in different photo-and thermoperiods in a phytotron as a basis for early selection.  
22 775 *Scand. J. Forest Res.* 10, 129-139. doi: 10.1080/02827589509382876
- 23 776 Nguyen, T.Q., and Emery, R.N. (2017). Is ABA the earliest upstream inhibitor of apical  
24 777 dominance? *J. Exp. Bot.* 68, 881-884. doi: 10.1093/jxb/erx028
- 25 778 Paiva, J.A., Garcés, M., Alves, A., Garnier-Géré, P., Rodrigues, J.C., Lalanne, C., et al. (2008).  
26 779 Molecular and phenotypic profiling from the base to the crown in maritime pine  
27 780 wood-forming tissue. *New Phytol.* 178, 283-301. doi: 10.1111/j.1469-8137.2008.02379.x
- 28 781 Pascual, J., Cañal, M.J., Escandón, M., Meijón, M., Weckwerth, W., and Valledor, L. (2017).  
29 782 Integrated physiological, proteomic, and metabolomic analysis of ultra violet (UV) stress  
30 783 responses and adaptation mechanisms in *Pinus radiata*. *Mol. Cell. Proteomics* 16, 485-  
31 784 501. doi: 10.1074/mcp.M116.059436
- 32 785 Penterman, J., Zilberman, D., Huh, J.H., Ballinger, T., Henikoff, S., and Fischer, R.L. (2007). DNA  
33 786 demethylation in the Arabidopsis genome. *Proc. Natl. Acad. Sci. U.S.A* 104, 6752-6757.  
34 787 doi: 10.1073/pnas.0701861104
- 35 788 Pluskal, T., Castillo, S., Villar-Briones, A., and Orešič, M. (2010). MZmine 2: modular framework  
36 789 for processing, visualizing, and analyzing mass spectrometry-based molecular profile  
37 790 data. *BMC Bioinformatics* 11, 395. doi: 10.1186/1471-2105-11-395
- 38 791 Ponting, C.P., and Aravind, L. (1999). START: a lipid-binding domain in StAR, HD-ZIP and  
39 792 signalling proteins. *Trends Biochem. Sci.* 24, 130-132. doi: 10.1016/s0968-  
40 793 0004(99)01362-6
- 41 794 Proost, S., Van Bel, M., Vaneechoutte, D., Van de Peer, Y., Inzé, D., Mueller-Roeber, B., et al.  
42 795 (2014). PLAZA 3.0: an access point for plant comparative genomics. *Nucleic Acids Res.*  
43 796 43, 974-981. doi: 10.1093/nar/gku986
- 44 797 R Development Core Team. (2015). *A Language and Environment for Statistical Computing:  
45 798 Vienna: R Foundation for Statistical Computing.*
- 46 799 Richards, D.E., King, K.E., Ait-Ali, T., and Harberd, N.P. (2001). How gibberellin regulates plant  
50 800 growth and development: a molecular genetic analysis of gibberellin signaling. *Ann.  
47 801 Rev. Plant Biol.* 52, 67-88. doi: 10.1146/annurev.arplant.52.1.67
- 48 802 Rivero, R.M., Ruiz, J.M., Garcia, P.C., Lopez-Lefebvre, L.R., Sánchez, E., and Romero, L. (2001).  
49 803 Resistance to cold and heat stress: accumulation of phenolic compounds in tomato and  
50 804 watermelon plants. *Plant Sci.* 160, 315-321. doi: 10.1016/S0168-9452(00)00395-2
- 51 805 Rocha, P.S., Sheikh, M., Melchiorre, R., Fagard, M., Boutet, S., Loach, R., et al. (2005). The  
52 806 Arabidopsis *HOMOLOGY-DEPENDENT GENE SILENCING1* gene codes for an S-  
53 807 adenosyl-L-homocysteine hydrolase required for DNA methylation-dependent gene  
54 808 silencing. *Plant Cell* 17, 404-417. doi: 10.1105/tpc.104.028332
- 55 809 Rohart, F., Gautier, B., Singh, A., and Lê Cao, K.-A. (2017). mixOmics: An R package for 'omics  
56 810 feature selection and multiple data integration. *PLoS Comput. Biol.* 13, e1005752. doi:  
57 811 10.1371/journal.pcbi.1005752
- 58 812 Romero-Rodríguez, M.C., Pascual, J., Valledor, L., and Jorrín-Novo, J. (2014). Improving the  
59 813 quality of protein identification in non-model species. Characterization of *Quercus ilex*  
60 814 seed and *Pinus radiata* needle proteomes by using SEQUEST and custom databases. *J.  
61 815 Proteomics* 105, 85-91. doi: 10.1016/j.jprot.2014.01.027

- 1  
2  
3 816 RStudio Team. (2016). *RStudio: Integrated development environment for R*. Boston, MA.
- 4 817 Ruffer, M., Nagakura, N., and Zenk, M.H. (1978). Strictosidine, the common precursor for  
5 818 monoterpene indole alkaloids with 3  $\alpha$  and 3  $\beta$  configuration. *Tetrahedron Lett.* 18,  
6 819 1593-1596. doi: 10.1016/S0040-4039(01)94613-1
- 7 820 Sabatier, S., Baradat, P., and Barthelemy, D. (2003). Intra- and interspecific variations of  
8 821 polycyclism in young trees of *Cedrus atlantica* (Endl.) Manetti ex. Carrière and *Cedrus*  
9 822 *libani* A. Rich (Pinaceae). *Ann. For. Sci.* 60, 19-29. doi: 10.1051/forest:2002070
- 10 823 Sadka, A., Dahan, E., Cohen, L., and Marsh, K.B. (2000). Aconitase activity and expression  
11 824 during the development of lemon fruit. *Physiol. Plantarum* 108, 255-262. doi:  
12 825 10.1034/j.1399-3054.2000.108003255.x
- 13 826 Sangster, T.A., and Queitsch, C. (2005). The HSP90 chaperone complex, an emerging force in  
14 827 plant development and phenotypic plasticity. *Curr. Opin. Plant Biol.* 8, 86-92. doi:  
15 828 10.1016/j.pbi.2004.11.012
- 16 829 Schmitz, A.J., Glynn, J.M., Olson, B.J., Stokes, K.D., and Osteryoung, K.W. (2009). *Arabidopsis*  
17 830 FtsZ2-1 and FtsZ2-2 are functionally redundant, but FtsZ-based plastid division is not  
18 831 essential for chloroplast partitioning or plant growth and development. *Mol. Plant* 2, 1211-  
19 832 1222. doi: 10.1093/mp/ssp077
- 20 833 Schrick, K., Bruno, M., Khosla, A., Cox, P.N., Marlatt, S.A., Roque, R.A., et al. (2014). Shared  
21 834 functions of plant and mammalian StAR-related lipid transfer (START) domains in  
22 835 modulating transcription factor activity. *BMC Biology* 12, 70. doi: 10.1186/s12915-014-  
23 836 0070-8
- 24 837 Sen, C.K., and Packer, L. (1996). Antioxidant and redox regulation of gene transcription. *Faseb*  
25 838 *J.* 10, 709-720. doi: 10.1096/fasebj.10.7.8635688
- 26 839 Shannon, P., Markiel, A., Ozier, O., Baliga, N.S., Wang, J.T., Ramage, D., et al. (2003).  
27 840 Cytoscape: a software environment for integrated models of biomolecular interaction  
28 841 networks. *Genome Res.* 13, 2498-2504. doi: 10.1101/gr.1239303
- 29 842 Singh, A., Gautier, B., Shannon, C.P., Rohart, F., Vacher, M., Tebutt, S.J., et al. (2018). DIABLO:  
30 843 from multi-omics assays to biomarker discovery, an integrative approach. *bioRxiv*. doi:  
31 844 10.1101/067611
- 32 845 Tanaka, H., Masuta, C., Uehara, K., Kataoka, J., Koiwai, A., and Noma, M. (1997). Morphological  
33 846 changes and hypomethylation of DNA in transgenic tobacco expressing antisense RNA  
34 847 of the S-adenosyl-L-homocysteine hydrolase gene. *Plant Mol. Biol.* 35, 981-986. doi:  
35 848 10.1023/A:1005896711321
- 36 849 Tariq, M., and Paszkowski, J. (2004). DNA and histone methylation in plants. *Trends Genet.* 20,  
37 850 244-251. doi: 10.1016/j.tig.2004.04.005
- 38 851 Thimm, O., Bläsing, O., Gibon, Y., Nagel, A., Meyer, S., Krüger, P., et al. (2004). MAPMAN: a  
39 852 user-driven tool to display genomics data sets onto diagrams of metabolic pathways and  
40 853 other biological processes. *Plant J.* 37, 914-939. doi: 10.1111/j.1365-313x.2004.02016.x
- 41 854 Treutter, D. (2005). Significance of Flavonoids in Plant Resistance and Enhancement of Their  
42 855 Biosynthesis. *Plant Biol.* 7, 581-591. doi:10.1055/s-2005-873009
- 43 856 Trontin, J.-F., Klimaszewska, K., Morel, A., Hargreaves, C., and Lelu-Walter, M.-A. (2016).  
44 857 "Molecular aspects of conifer zygotic and somatic embryo development: a review of  
45 858 genome-wide approaches and recent insights," in *In vitro embryogenesis in higher plants*.  
46 859 (Cham: Springer International Publishing AG), 167-207.
- 47 860 Uggla, C., Magel, E., Moritz, T., and Sundberg, B. (2001). Function and dynamics of auxin and  
48 861 carbohydrates during earlywood/latewood transition in Scots pine. *Plant Physiol.* 125,  
49 862 2029-2039. doi: 10.1104/pp.125.4.2029
- 50 863 Valdés, A.E., Fernández, B., and Centeno, M.L. (2004). Hormonal changes throughout  
51 864 maturation and ageing in *Pinus pinea*. *Plant Physiol. Bioch.* 42, 335-340. doi:  
52 865 10.1016/j.plaphy.2004.02.004
- 53 866 Valledor, L., Carbó, M., Lamelas, L., Escandón, M., Colina, F.J., Cañal, M.J., et al. (2018). "When  
54 867 the tree let us see the forest: systems biology and natural variation studies in forest  
55 868 species" in *Progress in Botany*, eds Cánovas F., Lüttge U., Leuschner C., and Risueño  
56 869 MC (Cham: Springer International Publishing AG), 353-375.
- 57 870 Valledor, L., Escandón, M., Meijón, M., Nukarinen, E., Cañal, M.J., and Weckwerth, W. (2014a).  
58 871 A universal protocol for the combined isolation of metabolites, DNA, long RNAs, small  
59 872 RNAs, and proteins from plants and microorganisms. *Plant J.* 79, 173-180. doi:  
60 873 10.1111/tbj.12546

- 1  
2  
3 874 Valledor, L., and Jorrín, J. (2011). Back to the basics: maximizing the information obtained by  
4 875 quantitative two dimensional gel electrophoresis analyses by an appropriate experimental  
5 876 design and statistical analyses. *J. Proteomics* 74, 1-18. doi: 10.1016/j.jprot.2010.07.007  
6 877 Valledor, L., Jorrín, J.s.V., Rodríguez, J.L., Lenz, C., Meijón, M., Rodríguez, R., et al. (2010a).  
7 878 Combined proteomic and transcriptomic analysis identifies differentially expressed  
8 879 pathways associated to *Pinus radiata* needle maturation. *J. Proteome Res.* 9, 3954-3979.  
9 880 doi: 10.1021/pr1001669  
10 881 Valledor, L., Meijón, M., Hasbún, R., Cañal, M.J., and Rodríguez, R. (2010b). Variations in DNA  
11 882 methylation, acetylated histone H4, and methylated histone H3 during *Pinus radiata*  
12 883 needle maturation in relation to the loss of in vitro organogenic capability. *J. Plant Physiol.*  
13 884 167, 351-357. doi: 10.1016/j.jplph.2009.09.018  
14 885 Valledor, L., Pascual, J., Meijón, M., Escandón, M., and Cañal, M.J. (2015). Conserved epigenetic  
15 886 mechanisms could play a key role in regulation of photosynthesis and development-  
16 887 related genes during needle development of *Pinus radiata*. *PLoS One* 10, e0126405. doi:  
17 888 10.1371/journal.pone.0126405  
18 889 Valledor, L., Romero-Rodríguez, M.C., and Jorrin-Novo, J.V. (2014b). "Standardization of data  
19 890 processing and statistical analysis in comparative plant proteomics experiment," in *Plant*  
20 891 *Proteomics*. (Cham: International Publishing Springer AG), 51-60.  
21 892 Valledor, L., and Weckwerth, W. (2014). "An improved detergent-compatible gel-fractionation LC-  
22 893 LTQ-Orbitrap-MS workflow for plant and microbial proteomics," in *Plant Proteomics:*  
23 894 *Methods and Protocols*. (Cham: Springer International Publishing AG), 347-358.  
24 895 Vázquez-González, C., López-Goldar, X., Zas, R., and Sampedro, L. (2019). Neutral and climate-  
25 896 driven adaptive processes contribute to explain population variation in resin duct traits in  
26 897 a mediterranean pine species. *Front. Plant Sci.* 10, 1-12. doi: 10.3389/fpls.2019.01613  
27 898 Verdú, M., and Climent, J. (2007). Evolutionary correlations of polycyclic shoot growth in *Acer*  
28 899 (*Sapindaceae*). *Am. J. Bot.* 94, 1316-1320. doi: 10.3732/ajb.94.8.1316  
29 900 Vimont, N., Schwarzenberg, A., Domijan, M., Beauvieux, R., Arkoun, M., Jamois, F., et al. (2019).  
30 901 Hormonal balance finely tunes dormancy status in sweet cherry flower buds. *bioRxiv*,  
31 902 423871. doi: 10.1101/423871  
32 903 Vizcaíno-Palomar, N., Ibáñez, I., González-Martínez, S.C., Zavala, M.A., and Alía, R. (2016).  
33 904 Adaptation and plasticity in aboveground allometry variation of four pine species along  
34 905 environmental gradients. *Ecol. Evol.* 6, 7561-7573. doi: 10.1002/ece3.2153  
35 906 Wang, W., Vinocur, B., Shoseyov, O., and Altman, A. (2004). Role of plant heat-shock proteins  
36 907 and molecular chaperones in the abiotic stress response. *Trends Plant Sci.* 9, 244-252.  
37 908 doi: 10.1016/j.tplants.2004.03.006  
38 909 Woo, E.-J., Dunwell, J.M., Goodenough, P.W., Marvier, A.C., and Pickersgill, R.W. (2000).  
39 910 Germin is a manganese containing homo-hexamer with oxalate oxidase and superoxide  
40 911 dismutase activities. *Nat. Struct. Mol. Biol.* 7, 1036. doi: 10.1038/80954  
41 912 Zas, R., and Fernández-López, J. (2005). Juvenile genetic parameters and genotypic stability of  
42 913 *Pinus pinaster* Ait. open-pollinated families under different water and nutrient regimes.  
43 914 *For. Sci.* 51, 165-174. doi: 10.1093/forestscience/51.2.165  
44 915 Zas, R., Merlo, E., and Fernández-López, J. (2004). Genetic parameter estimates for Maritime  
45 916 pine in the Atlantic coast of North-west Spain. *For. Genet.* 11, 45-53. doi: 10261/101373  
46 917 Zhang, C.-J., Zhao, B.-C., Ge, W.-N., Zhang, Y.-F., Song, Y., Sun, D.-Y., et al. (2011). An  
47 918 apoplastic h-type thioredoxin is involved in the stress response through regulation of the  
48 919 apoplastic reactive oxygen species in rice. *Plant Physiol.* 157, 1884-1899. doi:  
49 920 10.1104/pp.111.182808  
50 921 Zheng, C., Halaly, T., Acheampong, A.K., Takebayashi, Y., Jikumaru, Y., Kamiya, Y., et al. (2015).  
51 922 Abscisic acid (ABA) regulates grape bud dormancy, and dormancy release stimuli may  
52 923 act through modification of ABA metabolism. *J. Exp. Bot.* 66, 1527-1542. doi:  
53 924 10.1093/jxb/eru519  
54 925 Zhu, H., Qian, W., Lu, X., Li, D., Liu, X., Liu, K., et al. (2005). Expression patterns of purple acid  
55 926 phosphatase genes in *Arabidopsis* organs and functional analysis of *AtPAP23*  
56 927 predominantly transcribed in flower. *Plant Mol. Biol.* 59, 581-594. doi: 10.1007/s11103-  
57 928 005-0183-0  
58 929 Zimmerman, J.L. (1993). Somatic embryogenesis: a model for early development in higher plants.  
59 930 *Plant Cell* 5, 1411. doi: 10.1105/tpc.5.10.1411  
60 931  
61 932

933

934 **FIGURE LEGENDS**

935 **Figure 1.** Plant material employed in this analysis. Two-year old seedlings exhibiting an apical  
936 bud with young (**A**) or mature (**B**) morphology. Comparison of [juvenileyoung](#) (left) and [adultmature](#)  
937 (right) buds (**C**). Dissection of [juvenileyoung](#) (left) and [adultmature](#) (right) buds into their apical  
938 and basal parts (**D**). Vertical bars represent 0.5 cm length.

939

940 **Figure 2.** Venn diagrams showing the qualitative differences between bud sections and ontogenic  
941 stages at proteome (**A**) and metabolome (**B**) levels. Heatmap clustering of proteins (**C**) and  
942 metabolites (**D**) classified according to Mapman categories. Distances were established  
943 employing Manhattan distance and aggregated according to Ward's method.

944

945 **Figure 3.** Integrative analysis of proteome and metabolome. (**A**) Plot of samples scores at  
946 proteome and metabolome levels, showing components 1 and 2 in horizontal and vertical axes,  
947 respectively, (**B**) integrative heatmap clustering, (**C**) loadings plot showing the proteins with  
948 greatest correlation to components 1 and 2, (**D**) and loadings plot showing the metabolites with  
949 greatest correlation to components 1 and 2. Color code of the horizontal bar of the heatmap  
950 represents proteins (cyan) or metabolites (purple), while vertical shows treatments. Euclidean  
951 distances and complete-linkage algorithms were employed for classifying samples. Color of the  
952 protein loading bars represent the treatment with higher protein abundance.

953 **Figure 4.** Integrative analysis of proteome and metabolome during bud maturation. (**A**) sPLS-  
954 based network built after DIABLO analysis. Correlation cut-off was 0.75 and edge color reflect  
955 positive (red) or negative (green) interactions. Node color indicate Mapman functional bin and  
956 shape indicate proteins (circle) or metabolites (square). Same representations in which node color  
957 indicates that protein/metabolite is more abundant in (**B**) one of the treatments, (**C**) in the  
958 apical/basal part of the bud, or (**D**) in [adultmature](#)/[juvenileyoung](#) buds.

959 **Figure 5.** Whisker box representation of the qPCR analysis of target genes in the different bud  
960 sections. Dots indicate expression values of the different biological replicates normalized vs the  
961 expression of control genes ( $\Delta\text{Cq Target}/\Delta\text{Cq Controls}$ ). Significant differences between bud  
962 sections and developmental status (ANOVA/Tukey HSD,  $p < 0.001$ ) were highlighted (\*\*\*)

963

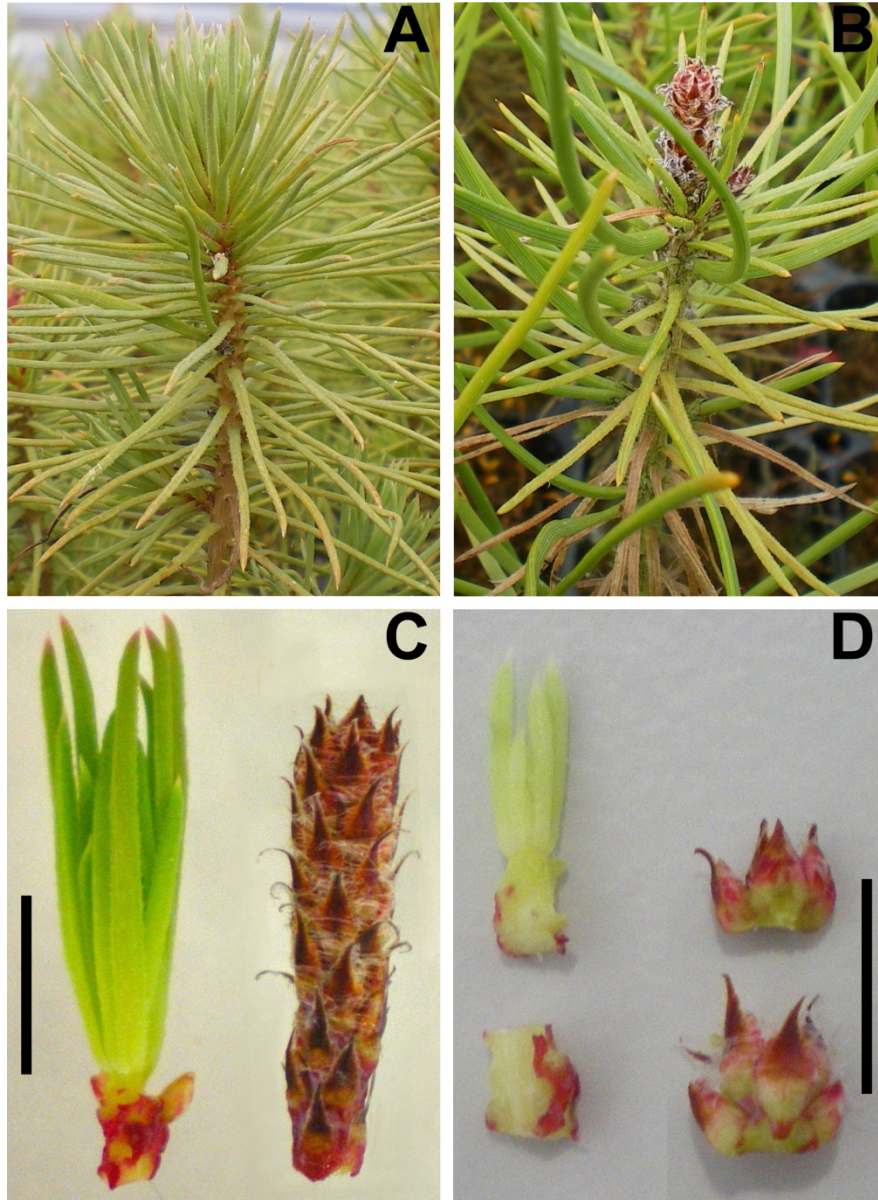


Figure 1. Plant material employed in this analysis. Two-year old seedlings exhibiting an apical bud with young (A) or mature (B) morphology. Comparison of juvenile (left) and adult (right) buds (C). Dissection of juvenile (left) and adult (right) buds into their apical and basal parts (D). Vertical bars represent 0.5 cm length



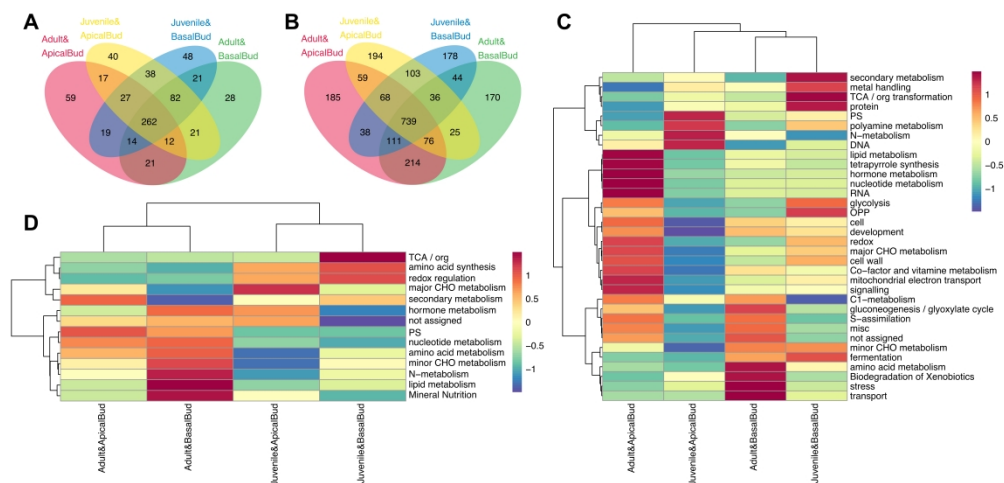


Figure 2. Venn diagrams showing the qualitative differences between bud sections and ontogenic stages at proteome (A) and metabolome (B) levels. Heatmap clustering of proteins (C) and metabolites (D) classified according to Mapman categories. Distances were established employing Manhattan distance and aggregated according to Ward's method.

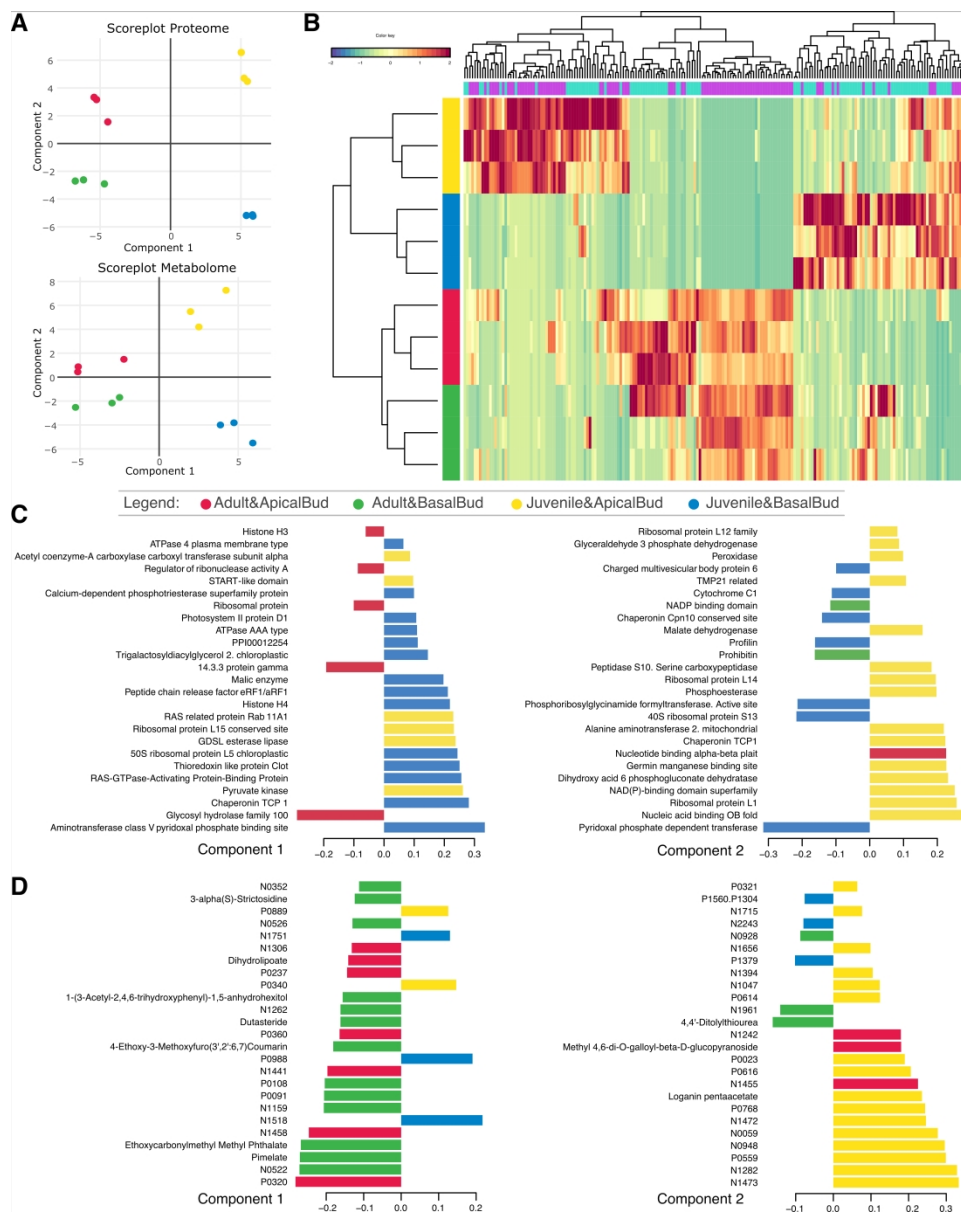


Figure 3. Integrative analysis of proteome and metabolome. (A) Plot of samples scores at proteome and metabolome levels, showing components 1 and 2 in horizontal and vertical axes, respectively, (B) integrative heatmap clustering, (C) loadings plot showing the proteins with greatest correlation to components 1 and 2, (D) loadings plot showing the metabolites with greatest correlation to components 1 and 2. Color code of the horizontal bar of the heatmap represents proteins (cyan) or metabolites (purple), while vertical shows treatments. Euclidean distances and complete-linkage algorithms were employed for classifying samples. Color of the protein loading bars represent the treatment with higher protein abundance.

421x527mm (300 x 300 DPI)

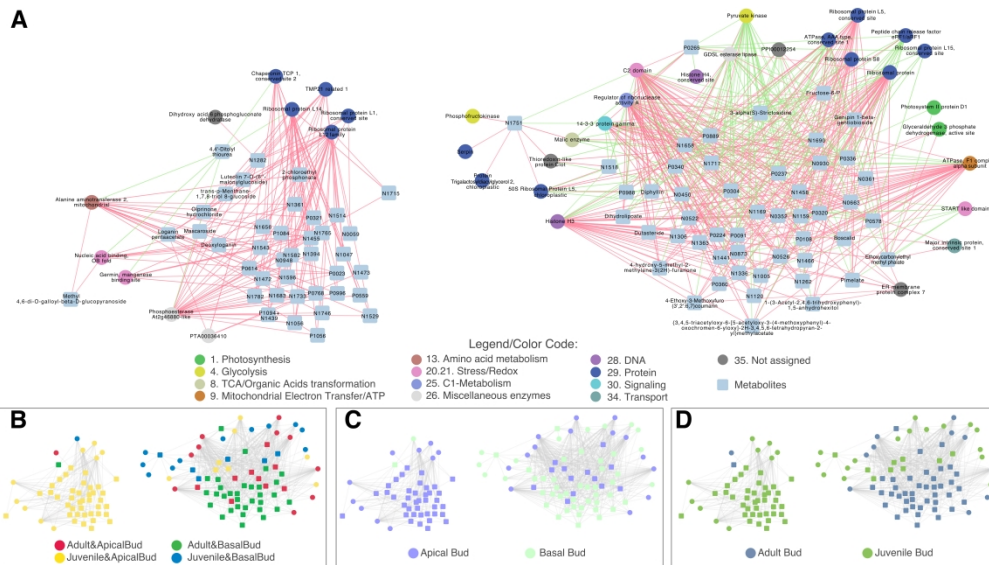


Figure 4. Integrative analysis of proteome and metabolome during bud maturation. (A) sPLS-based network built after DIABLO analysis. Correlation cut-off was 0.75 and edge color reflect positive (red) or negative (green) interactions. Node color indicate Mapman functional bin and shape indicate proteins (circle) or metabolites (square). Same representations in which node color indicates that protein/metabolite is more abundant in (B) one of the treatments, (C) in the apical/basal part of the bud, or (D) in adult/juvenile buds.

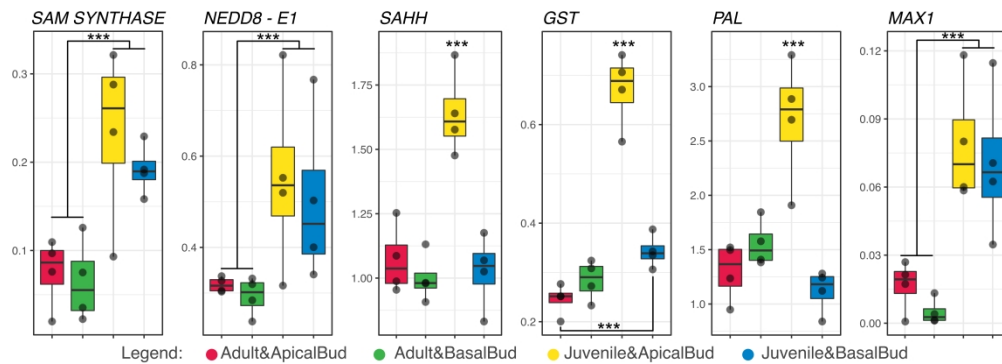


Figure 5. Whisker box representation of the qPCR analysis of target genes in the different bud sections. Dots indicate expression values of the different biological replicates normalized vs the expression of control genes ( $\square$ Cq Target/ $\square$ Cq Controls). Significant differences between bud sections and developmental status (ANOVA/Tukey HSD,  $p < 0.001$ ) were highlighted (\*\*\*).